ELSEVIER

Contents lists available at ScienceDirect

Chemical Geology

journal homepage: www.elsevier.com/locate/chemgeo





Cave monitoring in the Peruvian Andes reveals monsoon climate preserved in speleothem calcite

Elizabeth Olson^{a,*}, David P. Gillikin^a, Laura Piccirillo^a, Anouk Verheyden^a, Alexander Forsyth^a, Kirsten Litchfield^a, Hailey Stoltenberg^a, Avery Clavel^a, Maryam Ramjohn^a, Saliha Nazir^a, Pedro M. Tapia^b, Dylan Parmenter^c, Donald T. Rodbell^a

- ^a Department of Geosciences, Union College, Schenectady, USA
- b Biologia Department, Universidad Peruana Cavetano Heredia, Lima, Peru
- ^c Department of Earth Sciences, University of Minnesota, Minneapolis, USA

ARTICLE INFO

Editor: Karen Johannesson

Keywords:
South American summer monsoon
Karst cave
Hydrogeochemistry
Stable isotopes
Calcite

ABSTRACT

Speleothem paleoclimate records from the Peruvian Andes have been interpreted to reflect the strength of the South American monsoon. While these interpretations have been verified through comparison with other regional and global climate records, the mechanics of the cave environment that facilitate the preservation of this signal with such consistency remain unstudied. Here, we present four years of environmental data from Huagapo and Pacupahuain cave, and one year from Antipayarguna cave. The data reveal that the cave environment is very stable with little to no change in temperature and 100% relative humidity year-round. This stability in cave air is juxtaposed with the monsoonal drip water pulse that increases drip rates over 40 times on average across all seven monitored drip sites. Compared to the amount-weighted precipitation average δ^{18} O_{precip} value, the cave drip water $\delta^{18}O_{DW}$ values are evaporatively ¹⁸O enriched during infiltration through the soil/epikarst. As the monsoonal precipitation pulse fades and drip rates decrease, changes in the drip water chemistry (trace elements Mg/Ca and Sr/Ca, dissolved inorganic carbon $\delta^{13}C_{DW}$, and $\delta^{18}O_{DW}$ values) indicate that prior calcite precipitation (PCP) drives the trace element and $\delta^{13}C_{DW}$ variability. The $\delta^{13}C_c$ and $\delta^{18}O_c$ values of farmed slide calcite are highly variable. However, high drip rate and lower cave air pCO2 during the monsoon combine to increase calcite precipitation rates. This causes speleothem records from these caves to be weighted toward annual monsoon conditions. Calcite isotope values from actively growing stalagmite tops support this finding. These results suggest that speleothems from these caves are sensitive to changes in monsoon precipitation amount, because it determines the duration of the monsoon drip water pulse, and therein, the extent of dry season PCP. Further, these data indicate that heterogeneity in the dolomitic limestone massif causes offsets between the carbon isotopes and trace metal concentrations between the caves, highlighting the need to normalize these datasets when chronology-stacking these proxies.

1. Introduction

Speleothem paleoclimate records provide high-resolution archives of climatic change worldwide. Dating these records via U/Th produces chronologies with low age uncertainty (\sim 1%), facilitating the interpretation of changes from orbital to annual temporal scales (e.g., Baker et al., 2008; Cruz et al., 2009). To interpret past climatic change, these climate histories overwhelmingly rely on the relationship between modern atmospheric circulation and the oxygen isotope value of precipitation ($\delta^{18}O_{precip}$) that is imprinted on the $\delta^{18}O$ value of cave drip

water ($\delta^{18}O_{DW}$) and, ultimately, the $\delta^{18}O$ value of speleothem calcite ($\delta^{18}O_c$). Modern cave monitoring studies significantly improve our understanding of how atmospheric climate signals transfer to the cave environment. For example, investigations into the $\delta^{18}O_c$ to $\delta^{18}O_{precip}$ relationship in multiple regions have found correlations to precipitation amount, i.e., the amount effect, (e.g. Bar-Matthews et al., 2003; Cobb et al., 2007; Lases-Hernandez et al., 2019; Thatcher et al., 2020), the degree of rainout along the water vapor trajectory (Lachniet et al., 2012; Wolf et al., 2020), and changes in moisture source region (Fleitmann et al., 2003). In the absence of modern calibration studies, researchers

E-mail address: olsone2@union.edu (E. Olson).

^{*} Corresponding author.

often employ multiple speleothem proxies to verify climatic interpretations; the most common of these are trace element concentrations (Cruz et al., 2009), but in some cases, these proxies provide results that are inconsistent with isotope proxies (e.g. Liu et al., 2020). A modern understanding of cave dynamics can aid the interpretation of trace elements as increased concentrations can result from prior calcite precipitation (PCP) during drying in the overlying epikarst (Fairchild et al., 2000) or non-climatic factors such as limestone composition and dissolution dynamics (Pracný et al., 2019). While trace elements can have multiple sources of variability, carbon isotopes of speleothem calcite ($\delta^{13}C_c$) are equally complex and underutilized. The $\delta^{13}C_c$ value is measured simultaneously with oxygen isotope analysis; however, these data are rarely used because the values are impacted by many factors including atmospheric CO2, karst hydrology (PCP), the isotopic composition of overlying vegetation and changes in biological productivity (Breecker, 2017; Bühler et al., 2022; Fohlmeister et al., 2020). Despite the inherent complexity in $\delta^{13}C_c$ records, several studies have found that these data correlate with precipitation amount and $\delta^{18}O_c$ (Duan et al., 2021; Li et al., 2020; Meckler et al., 2012; Vaks et al., 2003). Monitoring studies have shown that $\delta^{13}C_c$ values are sensitive to precipitation and changes in water balance at some sites (Li et al., 2021) while, at others, long residence times of water in the epikarst and PCP can mask this relationship (Voarintsoa and Therre, 2022). Understanding the modern cave environment has enabled further interpretation of paleoclimate proxies and led to a proliferation of these types of validated records (Bar-Matthews et al., 1999; Chen et al., 2016; Hardt et al., 2010; Serrato Marks et al., 2021).

In South America, speleothem paleoclimate records from 29 caves are currently in the SISALv2 database (Comas-Bru et al., 2020). Yet, there are only a few modern cave monitoring papers from the continent, and none at high elevations (Cruz et al., 2005; Jaqueto et al., 2016; Sekhon et al., 2021). The lack of cave monitoring can lead to misinterpretation of speleothem archives. This was highlighted in a recent study by Ward et al. (2019), who found that only one of several cave Sr isotope records reflected South American summer monsoon (SASM) intensity over the Holocene. Interior continental sites within the Amazon Basin likely do not reflect SASM intensity, and these sites have been misinterpreted according to Ward et al. (2019). While most cave records of δ¹⁸O_c from South America are interpreted as reflecting the amount effect, this relation has not been verified by monitoring cave drip water. In contemporaneous records over the past 120 thousand years (kyr), a dipole has been present between the western and eastern sides of the continent (Deininger et al., 2019). The dipole creates wet conditions in the western Andes during periods of strong SASM and drought in the eastern Nordeste region of Brazil due to atmospheric subsidence over the region. However, the dipole is absent during episodic cold events in the North Hemisphere (Heinrich and Bond Events and the Little Ice Age) when proxies show wetter conditions throughout the continent (Deininger et al., 2019). The apparent collapse of the dipole has been explained by changes in the degree of moisture recycling (Wang et al., 2017), secondary moisture sources (Zhang et al., 2016), and differences in water residence times between cave sites (Wortham et al., 2017). A recent comparison of Holocene $\delta^{18}O_c$ and modern $\delta^{18}O_{precip}$ in precipitation by Campos et al. (2019) supports previous paleoclimates interpretations showing that isotope values reflect changes in precipitation amount throughout South America. However, further modeling of these data by Orrison et al. (2022) suggests that multiple factors other than precipitation amount govern isotopic variability including air mass trajectory history, sub-grid cell centers of deep convection, and atmospheric recycling. This uncertainty in our understanding of past speleothem records from South America needs to be addressed. To this end, we present a multiyear cave monitoring study of three caves from the Peruvian Andes.

To study the dominant factors influencing speleothem records in the Junín region of the Peruvian Andes and to evaluate the potential interand intra- cave stacking of these records over time, we report here an

extensive physical and chemical dataset geared toward establishing modern relationships between paleoclimate records and the contemporary cave environment including temperature, rainfall, and ventilation dynamics. In this study, we hypothesis that previous paleoclimate studies have found speleothem records of South American monsoon strength in the Junin area caves because conditions within the cave environment and karst hydrology facilitate the preservation of the monsoon season in cave calcite. To test this hypothesis, we analyze four years (2019-2023) of sensor observations from Huagapo and Pacupahuain caves (temperature, pressure, and relative humidity (RH)). We combine this information with one year of periodic drip water, calcite and cave air sampling from Huagapo, Pacupahuain, and Antipayarguna caves to test whether or not 1) there are seasonal changes in the drip water chemistry that correspond to changes in contemporaneously collected precipitation (amount and isotope values) or cave conditions (RH, drip rate, etc.), 2) farmed calcite and modern stalagmite isotope values reflect annual or seasonal conditions, and 3) records from these caves can be stacked even if there are systematic offsets between caves that might persist through time. We discuss these findings in the context of paleoclimate applications.

2. Study area

The study area is in the Andes Mountains of central Peru between the Coastal Batholith and the Eastern Cordillera within the Marañón Fold-Thrust belt (Fig. 1A). The area is the headwaters of the Amazon Basin, making it a vital drainage basin for South America. The cave systems are developing in the Triassic dolomitic limestone massif (INGEMMET, 2017). Tectonic activity is common in the region due to the subduction of the Nazca plate beneath the South American plate on the coast 160 km west of our study area. The cave sites are within the temperate climate zone, receiving 330 \pm 85 mm in annual rainfall, data from 2001 to 2022 at the Tarma met station averaged (Senamhi, https://www.se namhi.gob.pe/?&p=estaciones, 08-24-23). The SASM delivers 78% of annual rainfall between December and March during austral summer. Monsoonal moisture is driven by land-sea temperature contrast between the Atlantic Ocean and the South American continent (Garreaud et al., 2003). As the ITCZ moves southward during arboreal winter, water vapor evaporated over the Atlantic Ocean moves landward, and continental scale convection across the Amazon Basin results in moisture transport to the high Andes. Meanwhile, dry winters frequently result in drought throughout the region. The SASM intensity is modulated on interannual timescales by temperature changes in the Pacific due to the El Niño Southern Oscillation (ENSO). During the La Niña (cool) ENSO phase, enhanced easterly winds intensify the moisture transport from the Amazon, increasing rain in the region. The El Niño (warm) ENSO phase causes westerly wind intensification and blockage of eastern moisture, resulting in decreased rain in the region (Vuille and Werner,

The study area is between the montane puna grassland and the wetter forested montane shrubland at elevations below 3500 masl. Soil organic layer thickness averages 1 m in the region, although it can be highly variable due to landslides resulting from the high erosion rate and steep topography of the karst landscape (Zimmermann et al., 2010). Vegetation is dominated by C3 plants especially ichu grass (*Jarava ichu*) at high elevations above tree line, and polylepis trees (*Polylepis multijuga*) and shrubs at lower elevations (Powell et al., 2012).

Antipayarguna cave ($11^{\circ}16'S$, $75^{\circ}51'W$, 4050 masl) is 85 m long with a small stream running through it to the small entrance less than a meter wide and is shallow with only ~50 m of bedrock above the entrance (Fig.1). Pacupahuain Cave ($11^{\circ}15'S$, $75^{\circ}49'W$, 3800 masl) is 800 m in length with ~100 m of bedrock overburden (Fig.1). A stream runs along several sections, the entrance is narrow with a chimney climb at 20 m into the cave restricting airflow. Huagapo Cave ($11^{\circ}16'S$, $75^{\circ}47'W$, 3600 masl) is 2.8 km long, with ~500 m of bedrock overburden and a large river running much of its length year-round (Fig.1). Huagapo has several

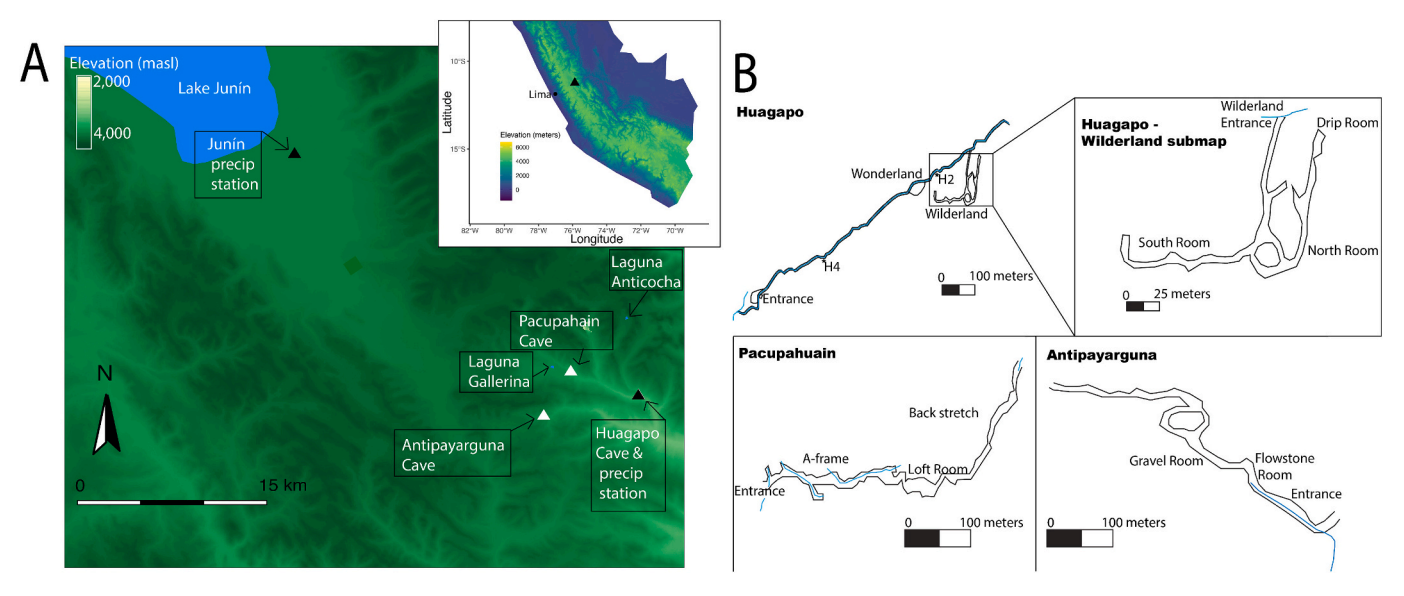


Fig. 1. Map of study area in the Peruvian Andes (A) and map of cave study sites (B). Cave maps are based on maps in (Sammartino et al., 1980). Sites H2 and H4 are temperature monitoring sites data shown in Fig. 3b.

large rooms with three siphons separating cave segments. The main entrance of Huagapo is large (~ 10 m), and the first 100-m section of the cave is easily walkable and open to tourists. Following the river into the cave, there are several low passes between sections (named Wonderland and Wilderland) that may restrict air flow. All data here are collected from the first 1 km section of the cave before the first siphon.

Huagapo and Pacupahuain caves have been the focus of several paleoclimatic studies that have demonstrated regional and global climate teleconnections on decadal to millennial scales (Burns et al., 2019; Burns et al., 2015; Kanner et al., 2013).

3. Materials and methods

3.1. Sensor data

Temperature, pressure, and relative humidity autonomous dataloggers (Onset) were installed in Huagapo and Pacupahuain caves in May 2019. In April 2022, additional dataloggers were installed in Huagapo and Pacupahuain caves, including Driptych Stalagmate drip counters (see SI Table 1 for sensor instrumentation details). In Antipayarguna Cave, a hand-held hygrometer and temperate sensor (KESTREL 5500) was used to take spot measurements while in the cave.

A rain gauge (Driptych Pluvimate), temperature, and pressure sensor (Onset) were installed outside Huagapo Cave in May 2019 (11°16′S, 75°47′W, 3500 masl). Huagapo precipitation was collected monthly from 2019 to 2022 and then weekly from 2022 to 2023. Precipitation was also collected monthly from 2019 to 2023 in the town of Junín (11°9′S, 75°59′W, 4115 masl). Rain gauge volume was recorded by citizen scientists at monthly sampling intervals. Precipitation samples were stored in 15 ml plastic centrifuge tubes (Falcon) until analysis.

To determine how and when changes in surface rainfall amount and relative humidity impact cave relative humidity and drip rate from 2019 to 2022, we use data from the nearby Tarma meteorological station (\sim 20 km SW of caves at 3100 masl). Rainfall amounts at the Tarma station closely matched the Pluvimate rain amounts recorded (2022–2023) at the Huagapo rain gauge ($r=0.57,\ n=404,\ p<0.0001$).

3.2. Sampling methods

Cave drip waters were collected over several days during four sampling trips in April 2022, June 2022, November 2022, and June 2023. At

each drip site, bulk drip water samples were collected at fast drips in 250 ml HDPE bottles, and slower drips were collected in 15 ml FalconTM tubes. Additionally, a Syp (Waitkato Scientific InstrumentsTM) automated fluid sampler system was installed in Pacupahuain Cave Loft 1, which collected samples every 72 h. All samples were filtered in the lab through 0.2 µm polyethersulfone syringe filters (Sartorius, 16,532-Q) and refrigerated until analysis. At several locations, bottles were left between trips and at hourly intervals during cave visits to collect time averaged drip waters. Where water volumes in the bottle were sufficient, a YSI meter was used to measure cave drip pH and temperature. These larger water samples were also filtered (0.2 µm) in the cave and stored in 50 ml Falcon™ tubes for total alkalinity analysis. The water samples for isotope and trace metal analysis were collected in 15 ml Falcon™ tubes. Drip water samples for δ^{13} C of dissolved inorganic carbon (DIC) were taken by directly collecting hanging drips with a syringe (or from reservoirs in time composite samples), then injecting 0.1 ml of water through the septa of a helium-flushed Exetainer® vial containing phosphoric acid. The Pacupahuain and Antipayarguna streams and Huagapo River were also sampled for the above parameters.

Cave air samples were collected in Exetainer® vials at each of the main study sites within the caves by first collecting air in a 10 ml syringe, then injecting it into the open vial and repeating it three times per vial. To prevent contamination from breath, air samples were taken by one individual slowly walking into the area alone and sampling before all other data collection commenced. Cave air pCO_2 concentrations in November 2022 were determined by collecting air in a 10 ml syringe in the cave and then measuring the samples on a PP Systems EGM-4 infrared CO_2 gas analyzer outside the cave, within several hours of collection. In June 2023 cave air pCO_2 concentrations were measured with colorimetric gas stain tubes and hand pump (Rae Systems).

Pre-scratched glass slides were placed below drips in each of the main study sites. Slides were harvested and replaced after each visit to the caves (~ 3 months) except for several left for the entire year of sampling (June 2022–June 2023). Four stalagmites from Huagapo-Wilderland with observed active drips were collected to obtain larger modern calcite samples.

To determine endmembers of trace metal and carbon sources, vegetation, bedrock, and soils were sampled above the caves.

3.3. Laboratory analysis

Stable water isotope analysis (δ^{18} O and δ^{2} H; VSMOW) was done via

cavity ring-down spectroscopy (L2140-*i* Picarro, USA) in high-precision mode. Briefly, 1.8 µl of filtered (0.2 µm) water was injected into the vaporization module heated to 110 °C; the sample volume was flushed with artificial air between analyses. Sample analysis consisted of 15 repeat analyses, followed by 20 min of integration time on each injection, and the average of the final five injections were used in calculating data to eliminate any memory effects between samples. Data were normalized to the SMOW-SLAP scale using USGS-47 and USGS-48 standards. The VSMOW2 reference standard was run (n=78) in each analysis to evaluate proper calibration to determine precision. Measurement precision reported as the standard deviation for δ^{18} O, and δ^{2} H is 0.08 and 0.54‰, respectively.

Stable isotope analysis of calcite, DIC, and air was conducted via isotope ratio mass spectrometry (IRMS) on a GasBench II coupled to a Thermo-Finnegan Delta Advantage IRMS following methods in Kelemen et al. (2017), Graniero et al. (2021), and Thermo Finnigan (2004) respectively. Approximately 80 µg of calcite was reacted with >99% phosphoric acid in He flushed Exetainers at 55 °C for at least 3 h. DIC isotopes were analyzed at room temperature (27 °C), and data were corrected for volume as described in Gillikin and Bouillon (2007). The last seven of eleven sample injections were averaged for calcite and DIC analysis. Air carbon isotopes were also analyzed at 27 °C, samples were injected eleven times, and the last five injection peaks were used. Data were normalized to the VPDB scale using IAEA 603 and NBS-18 standards for regression-based normalization. Precision for $\delta^{13}\text{C}$ and $\delta^{18}\text{O}$ is 0.06% (1 σ) or better based on analysis of IAEA 603 (n=40). Stable isotope analysis of soil and plant material was done using the same IRMS coupled to a Costech elemental analyzer via a Thermo ConFlo IV. Data were normalized to the VPDB scale using IAEA-N-2 and IAEA-600 standards. Precision for $\delta^{13}C$ is 0.05% (1 σ) or better based on analysis of IAEA-N-2 (n = 8).

Trace metal concentrations in drip water were determined by inductively coupled plasma - mass spectrometry (ICP-MS). Drip water samples were diluted to approximately 80 ppm Ca by adding 0.5 ml of filtered drip water to a 3 ml 1% HNO₃ solution prepared with trace metal grade HNO₃ and deionized water (>18 M Ω /cm). Samples were analyzed for Mg, Ca, and Sr on an Aglient™ 8900 Quadrupole Inductively Coupled Plasma- Mass Spectrometer (ICP-MS) following multiple-element standard-bracketing methods (Yu et al., 2005). Internal standards Sc and In at 100 ppb were added in-line via the autosampler during analysis. Calibration matrix-matched standards were run every ten samples created from gravimetrically prepared serial dilutions of Inorganic Ventures elemental stock solutions. Analytical precision was +/- 0.01 mmol/L (1 σ). Accuracy for drip water analysis was determined from the National Research Council Canada SLRS-6 (n = 70) and AQUA-1 (n = 70) 28) certified reference materials, the relative standard deviation was within 10% or less of reported values (see SI Table 2 for individual analyte information).

Total alkalinity was determined based on methods described in Bouillon et al. (2012, 2014) using a MetrOhm 888 TitrandoTM autotitrator and 869 compact sample changer with 0.1 mol l^{-1} HCl as titrant; reproducibility (1 σ) was typically better than $\pm 6~\mu mol~kg^{-1}$ based on 20 replicate analyses of an in-house standard.

3.4. Modern calcite modeling

The ISOLUTION model was used to predict the $\delta^{18}O_c$ and $\delta^{13}C_c$ values of calcite from sampled drip waters under observed cave conditions (Deininger et al., 2019). The model input parameters are included in the supplement (Table SI. 3) and do not include measured calcite data. Briefly, for each cave, the maximum and minimal observed values for the following parameters were used: temperature, relative humidity, drip rate, alkalinity, cave air pCO_2 , drip water $\delta^{18}O_{DW}$ and $\delta^{13}C_{DW}$ values. We use the temperature-dependent isotopic fractionation factor for water-calcite of -0.177%/°C from Tremaine et al. (2011) for cave calcite precipitation. The results of these model runs are then compared

to the observed isotope values of in-situ farmed calcite slides and modern stalagmite tops. By modeling the calcite from the drip water chemistry and sensor data alone, we can test our understanding of the cave system and the interpretation of calcite isotope values.

4. Results

4.1. Cave monitoring

Sensor data indicate that Huagapo and Pacupahuain cave temperature fluctuate more near the entrances and during the monsoon season (Fig.2). Exterior temperatures measured outside of Huagapo cave indicate that the average range of the diurnal cycle (24-h avg. = 11.2, σ = 6.0 °C) is greater than inter-seasonal variability (annual avg. = 11.2, σ =1.6 °C) (SI Fig.1). Temperature sensors at Huagapo entrance (100 m) show a prominent dip in temperatures at the onset of the monsoon season (November to mid-January). Internal cave temperatures at the Wonderland section of Huagapo Cave (avg = 10.9 σ = 0.1 $^{\circ}\text{C})$ show small seasonal increases in temperature during the monsoon (~ 0.3 °C). In contrast, the Wilderland Section of Huagapo Cave (avg = 10.7σ = 0.1 °C), the Loft Section of Pacupahuain Cave (avg =11.5 σ = 0.0 °C) and the Aframe Section of Pacupahuain Cave (avg =11.6, $\sigma = 0.0$ °C) temperature sensors show no change outside of sensor accuracy (0.2 °C) over the observed period (Figs. 2 & 3). The spot measurements of Antipayarguna – Gravel Room in June 2023 air temperature was 13.2 °C.

Cave relative humidity was 100% in most areas of Huagapo and Pacupahuain caves indicating that in-cave evaporation plays no role in water/calcite isotope fractionation. Cave relative humidity at Huagapo – Wilderland, Pacupahuain – Aframe, and Pacupahuain – Loft Room was 100% with no variation outside of the $\pm 2.5\%$ sensor accuracy (Fig. 3). However, relative humidity was not measured in the Wonderland area of Huagapo or Antipayarguna.

Cave pressure recorded in the caves is slightly lower compared to outside atmospheric pressure because of differences in the altitude of the sensors (Fig. 2). The mean outside Huagapo pressure 670 ($\sigma = 2$) hPa (3500 masl), is within sensor accuracy 6 hPa of inside Huagapo- Wilderland 667 ($\sigma = 2$) hPa (3600 masl) and is slightly higher than Pacupahuain–Loft Room 643 ($\sigma = 1$) hPa (3800 masl). Air pressure decreases with increasing elevation due to thickness of the overlying air column. Accounting for this offset in elevation between Pacupahuain and outside Huagapo, there is a 25 hPa difference due to elevation and, therefore, no difference between mean outside and in-cave pressure within sensor accuracy. Subtracting the mean from these pressure sensor series to account for these issues we see that the cave pressure is lower than surface pressure throughout the year (Fig. 3). Changes in outside atmospheric pressure are mirrored by cave air pressure at Pacupahuain-Loft/Aframe ($r^2 = 0.98$) and Huagapo–Wilderland ($r^2 = 0.96$), indicating diurnal exchange of air even though temperature and relative humidity remain constant. Pressure sensor data follow a diurnal cycle with high pressures at night and low pressures during the day. This diurnal cycle is present in both the in-cave and outside sensor time series (SI Fig. 3).

Drip rate at several sites in Huagapo and Pacupahuain caves increased during the monsoon season but lagged precipitation onset. Precipitation for the 2022–2023 year at the Huagapo cave rain gauge was similar to the reported historical average from the nearby city of Tarma, with a total rainfall of 500 mm and is seasonal with 63% falling during the monsoon between December and March. All drip counter data fall within the seepage flow category based on discharge and covariance under the Smart and Friedrich (1987) classification (SI. Fig. 4). Drip counter data indicate that the drip rate increases over 40-fold on average for the seven drip sites during the monsoon season compared to dry season conditions. Drip rate curves show flow along both matrix and fractured conduits within caves (Fig. 3), as classified in Treble et al. (2022). The drip rate response is synchronous; during the 2023 monsoon (December 2022 to April 2023), two fracture-fed drips in

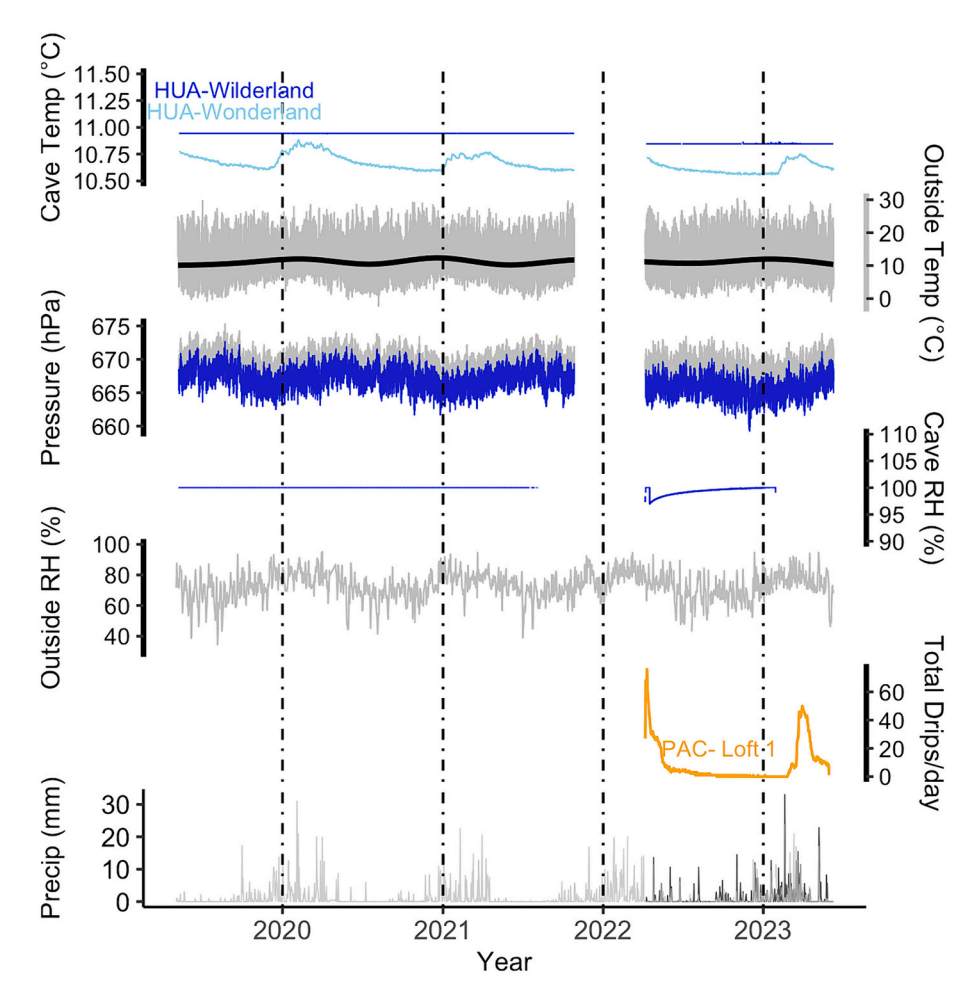


Fig. 2. Four years of monitoring data from outside and inside Huagapo and Pacupahuain caves. All data plotted in grey are from outside the caves, while inside parameters are plotted in color and coded by cave and study area (Pacupahuain – PAC is orange, Huagapo – HUA is blue for the Wilderland area and Wonderland is purple). Outside precipitation (grey) and relative humidity are from the nearest city of Tarma (Senamhi, https://www.senamhi.gob.pe/?&p=estaciones, 08–24-23). Additional precipitation data (black) is from a Pluvimate sensor at the station installed outside Huagapo cave. Outside pressure and temperature are from our meteorological station directly outside Huagapo Cave. Inside cave temperature from Huagapo Wilderland (blue) is from two overlapping temperature loggers. The drip rate is from a fracture-fed drip in Pacupahuain Loft-1. The gap in cave sensor data was due to a lack of access during the pandemic. (For interpretation of the references to color in this figure legend, the reader is referred to the web version of this article.)

Pacupahuain and one in Huagapo cave resumed on the same day (February 21st, 2023).

4.2. δ^{18} O and d-excess of precipitation and drip water

The $\delta^{18}O_{DW}$ and d-excess values of drip water are higher than annual amount-weighted precipitation values. Precipitation isotope values at the two precipitation sampling sites, Junín (avg. $\delta^{18}O_{precip} = -15.6$, $\sigma =$ 6.0%; avg. d-excess = 12.0, σ = 0.2%) and Huagapo (avg. δ ¹⁸O_{precip} = -14.4, $\sigma = 7.0\%$; avg. d-excess = 8.2, $\sigma = 3.7\%$) are offset with the higher elevation Junín site (4115 masl) being 1.2 % lower than the station directly outside Huagapo cave (3500 masl). These time series show similar trends over the year, with lowest isotope values in the monsoon season (Fig. 4). Precipitation isotopes decrease with increasing rain amount ($r^2 = 0.58$, n = 66, p < 0.0001). Drip water in the caves falls along a local evaporation line with the Antipayarguna being the least evaporated and Pacupahuain being the most evaporated. A sinkhole lake, Laguna Gallerina (3900 masl, area = 1 km²), is located above Pacupahuain cave (3800 masl). The water isotope values ($\delta^{18}O =$ -11.2%, d-excess = 4.2) show that the lake water was evaporated (during June 2023 sampling), this sample plots on the far end of the local evaporation line (Fig. 5).

The $\delta^{18}O_{DW}$ and d-excess drip water 2022–2023 time series from the

Syp autosampler in Pacupahuain cave compared with precipitation over the year show that drip water isotope values mirror precipitation variation over the year with some degree of lag time between the two timeseries. The Syp autosampler was set to collect drips over a 72 h window, and vials were empty from August to February. Then, in late February, the drips resumed filling all remaining vials in the carousel (the Syp malfunctioned and continuously sampled all drips instead of moving to the next sample position after 72 h). The Syp $\delta^{18}O_{DW}$ time series increases +2.0% during August 2022; at that time $\delta^{18}O_{precip}$ is 9% higher than the amount-weighted mean value. In contrast, the drip waters collected during an intermittent sampling trip in April 2022 during the monsoon drip water pulse show a much smaller increase (Fig. 5). Between April 2022 and June 2023 there was a small increase in the difference between $\delta^{18}O_{DW}$ drip water averages for Antipayarguna (+0.4%), Pacupahuain (+0.3%), and Huagapo (+0.2%). While precipitation $\delta^{18}O_{precip}$ over the year was highly variable ($\sigma=7\%$), the $\delta^{18}O_{DW}$ values fall within a much smaller range over the year with the standard deviation between all trips $\delta^{18}O_{DW} < 0.4$ (Table 1).

4.3. Cave air CO_2 $\delta^{13}C_{air}$ and pCO_2 concentration seasonal changes

Cave air pCO $_2$ was measured in November 2022 and June 2023 for Huagapo-Wilderland/Wonderland, Pacupahuain-Aframe/Loft Room

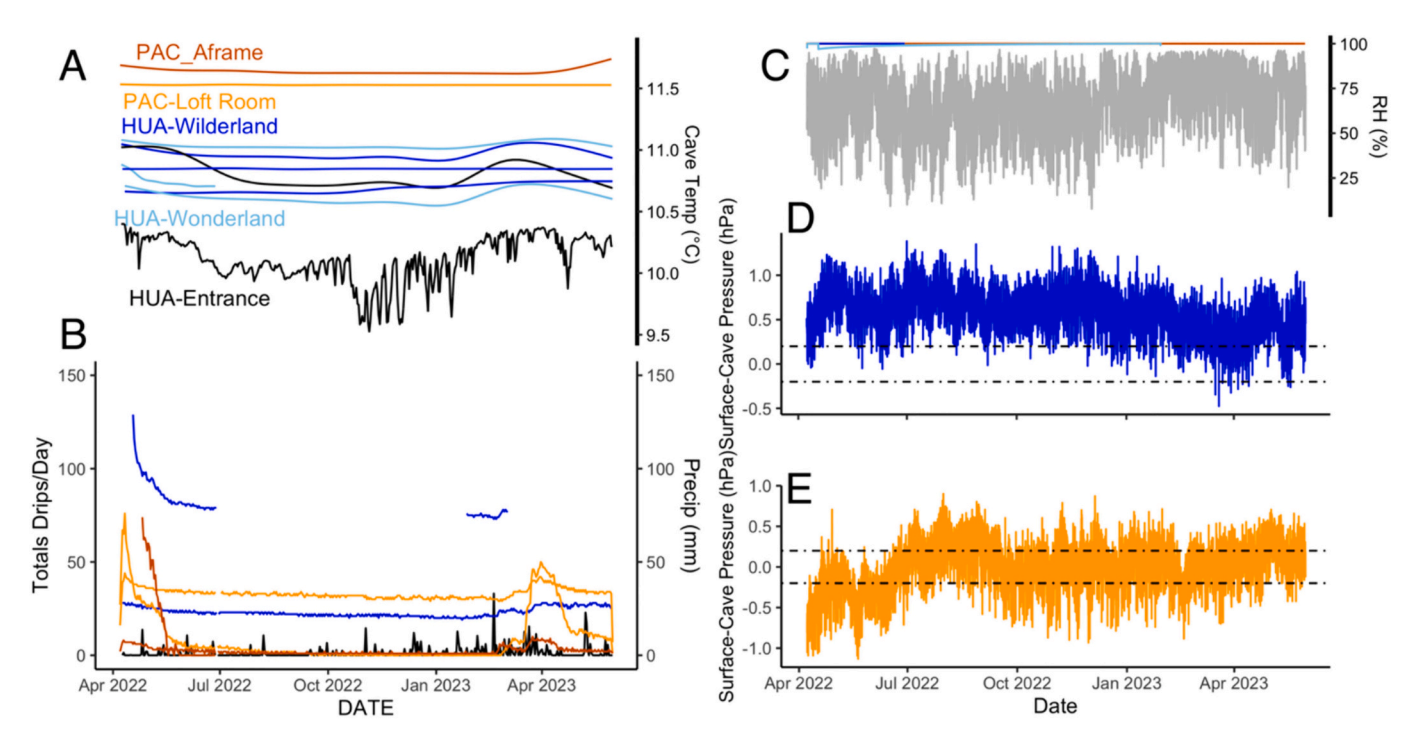


Fig. 3. Sensor data for the 2022–2023 year. A) Temperature data for Huagapo and Pacupahuain. Huagapo temperature data along transect from entrance (black) to Wonderland (purples) and Wilderland (blues). Pacupahuain temperature data for Aframe (red) and Loft 1 (yellow). B) Drip rate per day for two drip sites in Huagapo Wilderland (blues), four drip sites in Pacupahuain Loft 1 (yellows) and Aframe (reds) shown with precipitation from outside Huagapo (grey). C) Relative humidity inside (red) and outside (grey) the caves. D) Pressure Outside Huagapo minus inside Huagapo—Wilderland (blue). E) Pressure Outside Huagapo minus inside Pacupahuain–Loft Room (orange). Panels D and E have the mean removed from the data series shown in Fig. 2; sensor resolution range is denoted by the dotted black lines. Precipitation from outside Huagapo. The relative humidity data are overlapping from two sensors in Pacupahuain Loft 1 and Aframe and two sensors in Huagapo Wilderland they do not deviate from 100% outside of sensor accuracy. The offset between Huagapo and Pacupahuain pressure is due to the elevation difference of 200 m. Inside cave pressure mirrors outside cave pressure in time. (For interpretation of the references to color in this figure legend, the reader is referred to the web version of this article.)

and in Antipayarguna during June 2023. In Huagapo and Pacupahuain the $p\text{CO}_2$ values are higher in November than June. But this does not correspond with a change in the $\delta^{13}\text{C}_{air}$ of cave air CO_2 .

The $\delta^{13}C_{air}$ values of cave air CO_2 were measured during each of the four intermittent sampling trips. Changes in $\delta^{13}C_{air}$ values between seasons are small (1–1.5‰) indicating that cave ventilation is likely a diffuse gradual process (Figs. 6 and 7). The $\delta^{13}C_{air}$ values are lowest during the monsoon when soil biological activity is at its peak.

4.4. Mean calcite $\delta^{18}O_c$ and $\delta^{13}C_c$ differences between caves

To determine the main controls on calcite oxygen isotope values $(\delta^{18}O_c)$ we compared farmed calcite values with $\delta^{18}O_{DW}$ of drip water H_2O and $\delta^{18}O_{\textit{precip}}$ at our two stations along the same elevation gradient as the caves (Table 1). While the precipitation data show an small negative shift in $\delta^{18}O_{\textit{precip}}$ with increasing elevation the calcite $\delta^{18}O_c$ do not. The difference between the three caves average drip water $\delta^{18}O_{DW}$ is small (0.8‰, VSMOW). Similarly, the calcite $\delta^{18}O_c$ values overlap. However, the calcite $\delta^{18}O_c$ range (4‰, VPDB) is much larger than that of drip water.

To determine the main controls on calcite carbon isotope values, we compared farmed values with $\delta^{13}C_{DW}$ of drip water DIC, cave-air CO₂, bedrock, and soil carbon (Table 2). The cave calcite $\delta^{13}C_c$ is offset between the cave sites. There is no difference in vegetation $\delta^{13}C$ sampled around and above the caves. The dark micritic limestone bedrock sampled within and outside of Huagapo and Pacupahuain caves averages +1%. Antipayarguna cave is located at the contact between the Pucara and Mitu group. The Mitu group is comprised of red sandstones, with $\delta^{13}C_{BR}$ around -12% the carbonate cement in these sandstones is closer in value to farmed calcite from the cave (avg = -6.9%) than the Pucara carbonate bedrock (avg = +1%.). This likely reflects the ongoing

calcite deposition of Pucara carbonate on the poorly consolidated eroding Mitu sandstone bedrock unit. Therefore, the Pucara group is the dominant bedrock unit and has a consistent $\delta^{13}C_{BR}$ value. The $\delta^{13}C_{air}$ value of cave air CO $_2$ is +3% higher in Huagapo (avg =-16.2%) than the other two caves (avg =-19.0%), despite the soil and vegetation samples from around the caves being nearly identical in $\delta^{13}C$ (avg =-26.0%, $\sigma=1.6$) (SI Fig. 2). A similar offset is observed in the $\delta^{13}C_{DW}$ of drip water DIC with Huagapo values being +3.5% higher than Pacupahuain and Antipayarguna.

4.5. Bedrock source mixing and seasonal prior calcite precipitation (PCP)

The dolomitic limestone massif is heterogenous with respect to common trace elements (Mg and Sr) between study sites. However, in individual cave areas the host rock trace element ratios are constant, with the exception of drip waters from the Huagapo - Wilderland South Room. To calculate the limestone versus dolostone contribution to trace elements in drip waters we use the end-members for bedrock in Tremaine and Froelich (2013) and the mixing lines for constant Sr and Mg partition coefficients based on measured cave temperature and equations in Wassenburg et al. (2020). Bedrock for drip water flow paths ranges from 20 to 90% limestone in Huagapo cave, Pacupahuain cave is less variable with 65-85% limestone, and Antipayarguna cave is 30-20% limestone (Fig.8). The Huagapo Wonderland drip waters are 90% limestone. The two outlier samples, which plot near the Huagapo-Wilderland average drip waters are both from the H2 stream bed drip site (Fig. 1) that is between Wonderland and Wilderland. Actively growing stalagmites on the Wonderland loft and adjacent stream ledges therefore do not have a heterogenous bedrock source. In contrast, Huagapo-Wilderland has a large range of values from 30 to 75% limestone however, this range comes from a specific section of

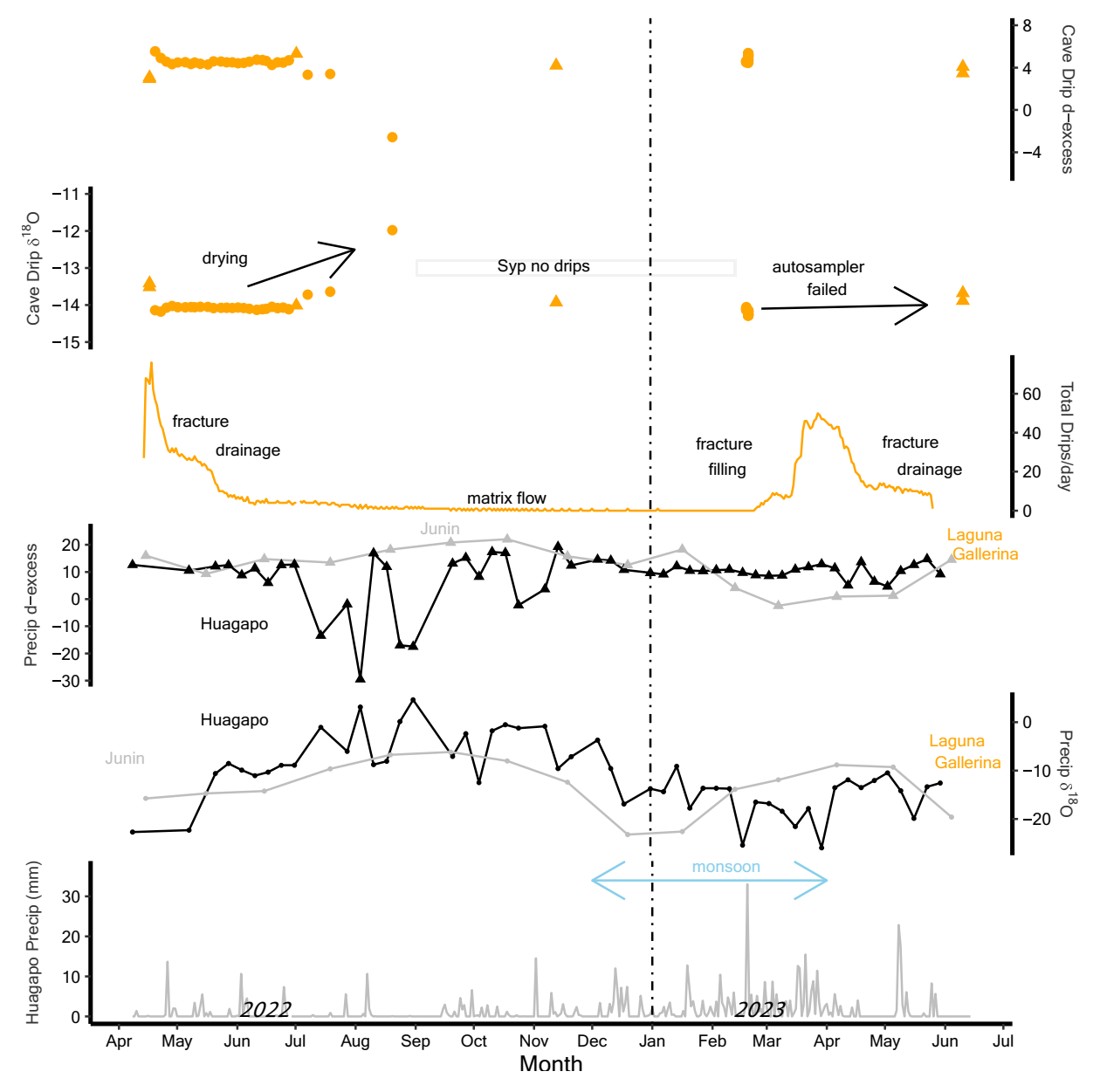


Fig. 4. Drip water and precipitation amount and water isotope data (in ‰) over the 2022–2023 sampling period. The monsoon period is highlighted by the vertical lines. The drip water isotope data come from the Syp autosampler in Pacupahuain Loft 1, from August 2022 to February 2023 there were no drips. Drips resumed on February 20, 2023, causing the autosampler to fail. Drip rate is plotted from an adjacent fracture fed drip also located on Loft 1.

Huagapo—Wilderland- South Room. All samples with <60% limestone are from the South Room, while Drip Room and North Room fall within the smaller 70–60% limestone range.

Increasing values along the ln Mg/Ca and ln Sr/Ca mixing lines (Fig. 8) indicate that PCP occurs at each site. Pacupahuain–Loft Room shows the greatest extent of PCP while Pacupahuain–Aframe and Huagapo–Wonderland also show a wide PCP extent. In contrast, Huagapo–Wilderland and both areas in Antipayarguna shows a much smaller range in PCP extent.

Intermittent sampling time series of trace elements indicate that the timing of peak prior calcite precipitation occurs during the dry season (Figs. 6 and 7). The increased values in Mg/Ca occur along with peaks in $\delta^{18}O_{DW}$ and $\delta^{13}C_{DIC}$ values indicative of PCP in drip water at the sites. The PCP peak occurs in the dry season at both Pacupahuain and Huagapo cave (June–November). The Pacupahuain-Loft Room Syp autosampler series caught this transition at its onset at that site for those

drips feeding into the autosampler funnel.

4.6. $\delta^{18}O_c$ and $\delta^{13}C_c$ of seasonally farmed calcite

The measured isotopic composition of in-situ farmed calcite differ from the ISOLUTION model output (Fig.9). Farmed calcite slides, in many cases, plot outside of the expected ISOLUTION modeled values for equilibrium calcite precipitation based on sensor and chemistry dripwater data inputs. The model data predict that the $\delta^{13}C_c$ values for Antipayarguna and Pacupahuain caves should be lower than those measured. Measured Huagapo cave $\delta^{13}C_c$ values fall within the modeled range. For $\delta^{18}O_c$ values, we find that there is a much larger range of values measured than the model predicts suggesting that disequilibrium processes are active throughout all caves over the course of the year.

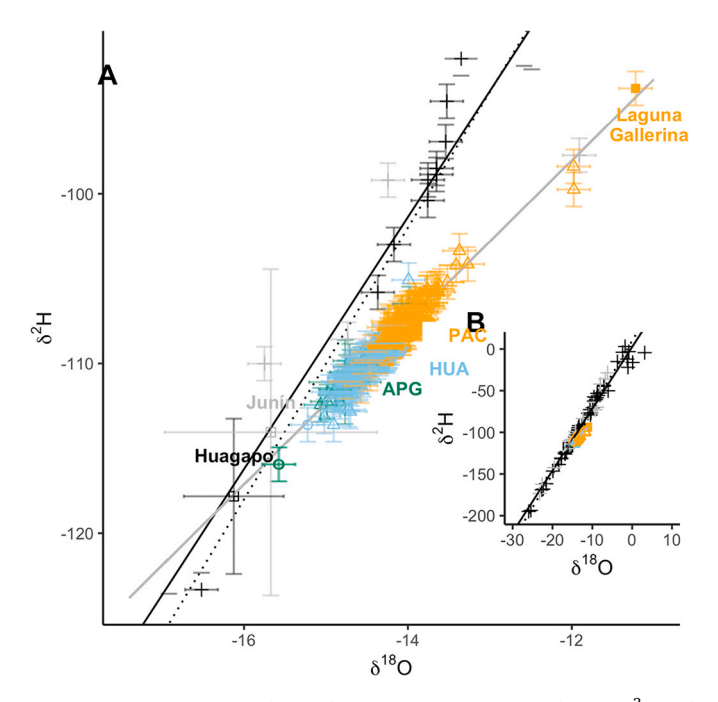


Fig. 5. Cave drip water and outside precipitation isotope values in $\delta^2 H$ and $\delta^{18}O$ space (in ‰). In panel A, the local meteoric water line (dotted black, LMWL) plots near the global meteoric water line (solid black, GMWL), the LMWL is $\delta^2 H=7.4 \ x \ \delta^{18}O+2.5.$ The cave drip waters fall along the local evaporation line (grey), $\delta^2 H=4.77 \ x \ \delta^{18}O$ -40.8. Panel B is the same as A but zoomed out to show full range of precipitation isotope data, box outlines extent of plot A within B.

5. Discussion

5.1. Seasonal changes in the cave environment

5.1.1. Cave ventilation and pCO₂

Previous cave monitoring studies show that cave venting events can cause abrupt changes in air circulation leading to decreases in relative humidity, favoring evaporation and increasing $\delta^{18}O_c$ values (Fairchild and Baker, 2012). Likewise, venting can lower cave air pCO_2 , causing calcite precipitation rates to increase (e.g. Oster et al., 2012), which leads to incomplete exchange between air and drip water pCO_2 prior to calcite precipitation resulting in higher $\delta^{13}C_c$ values. For this reason, understanding cave ventilation processes at a site is critical (Fairchild et al., 2006). In convective caves, ventilation causes large swings in cave air conditions that typically occur during winter when colder denser air sinks into the cave displacing warmer cave air (Gomell and Pflitsch, 2022). Tropical caves may not follow this predictable model because diurnal temperature fluctuations are greater than seasonal changes (James et al., 2015) or in other cases, water saturation of the epikarst in

monsoon regimes prevents seasonal ventilation and leads to CO2 accumulation irrespective of temperature changes (Bernal et al., 2023). In our study, we found that Huagapo and Pacupahuain caves are at slightly higher pressure than the surface. This overpressure should result in a slight pressure gradient (1 hPa) between the outside atmosphere and the cave inducing air flow out of the caves (Fig. 3). At Huagapo-Wonderland we see a slight increase in the temperature during the monsoon (Fig. 2). The increased temperature may be from increased atmospheric cave air exchange at that time. Alternatively, this heat signature may be from the drip water pulse as water enters the cave during the monsoon. The temperature fluctuations at the entrance to Huagapo indicate air circulation and thermal advection (Fig. 3). This effect is dampened within the first 300 m of the cave where temperature becomes invariable when thermal conduction likely controls cave temperature (Domínguez-Villar et al., 2023). While the physical process of air exchange in these caves warrants further investigation, the constant temperature and relative humidity data sets suggest a very stable cave environment with no abrupt events in the time series.

Seasonal shifts in cave air circulation and drip water chemistry alter the rate of calcite precipitation and therein can lead to large geochemical variability in dynamically ventilated cave systems. The geochemical properties of stalagmites are impacted, because in these systems calcite precipitation may outpace solute equilibration of species in the precipitating water film to varying degrees as cave air and drip water chemistry change. How calcite precipitation rates will differ in response to seasonal changes in the cave environment can be quantified using the equation from Dreybrodt and Fohlmeister (2022):

$$F = \alpha \left(c_{ca} - K(T) \sqrt[3]{p_{CO2}} \right)$$

Where calcite precipitation rate (F) is a function of the precipitation constant α , the concentration of calcium in drip water (c_{ca}) in mmol/L, the constant K, the concentration of cave air pCO_2 in atm (p_{CO2}) and temperature in degrees Celsius (T). The constants are temperature dependent K = -0.16 x T + 11.13 and $\alpha = 0.52 + 0.04$ T + 0.004 T² * 10^{-5} , where T is in degrees Celsius. Using this equation, we see that increased calcium concentrations and decreased cave air pCO2 favor higher precipitation rates in general. For these calculations, we assume a water film thickness typical for speleothem surfaces of 0.01 cm. The average precipitation rates for Huagapo and Pacupahuain caves are higher in June 2023 than in November 2022. Huagapo-Wonderland is 30% higher in June 2023 right after the wet season (9.5 \times 10⁻¹¹ cm³/s) as compared to November 2022 at the end of the dry season (6.9 \times 10⁻¹¹ cm³/s). While, Pacupahuain–Aframe is 50% greater in June 2023 $(2.2 \times 10^{-10} \text{ cm}^3/\text{s})$ compared to November 2022 $(1.1 \times 10^{-10} \text{ cm}^3/\text{s})$. June growth rates at Huagapo–Wilderland (6.8 \times 10⁻¹¹ cm³/s) and Pacupahuain–Loft (6.6 \times 10⁻¹¹ cm³/s) are 100% greater than November 2022 when dissolution conditions likely occur due to very high pCO_2 in those areas. While we do not have measured monsoon pCO2 values, we can infer that the concentration drops between November and June. Further, the monsoon February Syp autosampler drip waters from the

Table 1Isotope values of cave drip water and calcite samples.

Cave Area	Water, % VSMOV	Calcite, ‰ VPDB							
	Avg. δ ¹⁸ O _{DW}	$\sigma \delta^{18} O_{DW}$	Avg. $\delta^2 H_{DW}$	$\sigma \\ \delta^2 H_{DW}$	Avg. d-excess	n	Avg. δ ¹⁸ O _c	$^{\sigma}_{\delta^{18}O_c}$	n
Antipayarguna									
Flowstone Room	-14.7	0.4	-110	2.0	7.6	7	_	_	_
Gravel Room	-14.6	0.2	-109	0.7	7.8	7	-12.5	1.6	5
Huagapo									
Wilderland	-14.4	0.2	-109	0.9	6.2	67	-10.4	2.9	10
Wonderland	-14.8	0.2	-111	1.2	7.4	26	-12.0	1.3	5
Pacupahuain									
Aframe Room	-14.0	0.2	-106	1.2	6.0	17	-9.2	2.8	13
Loft Room	-14.0	0.3	-110	1.2	2.0	114	-8.5	2.0	10

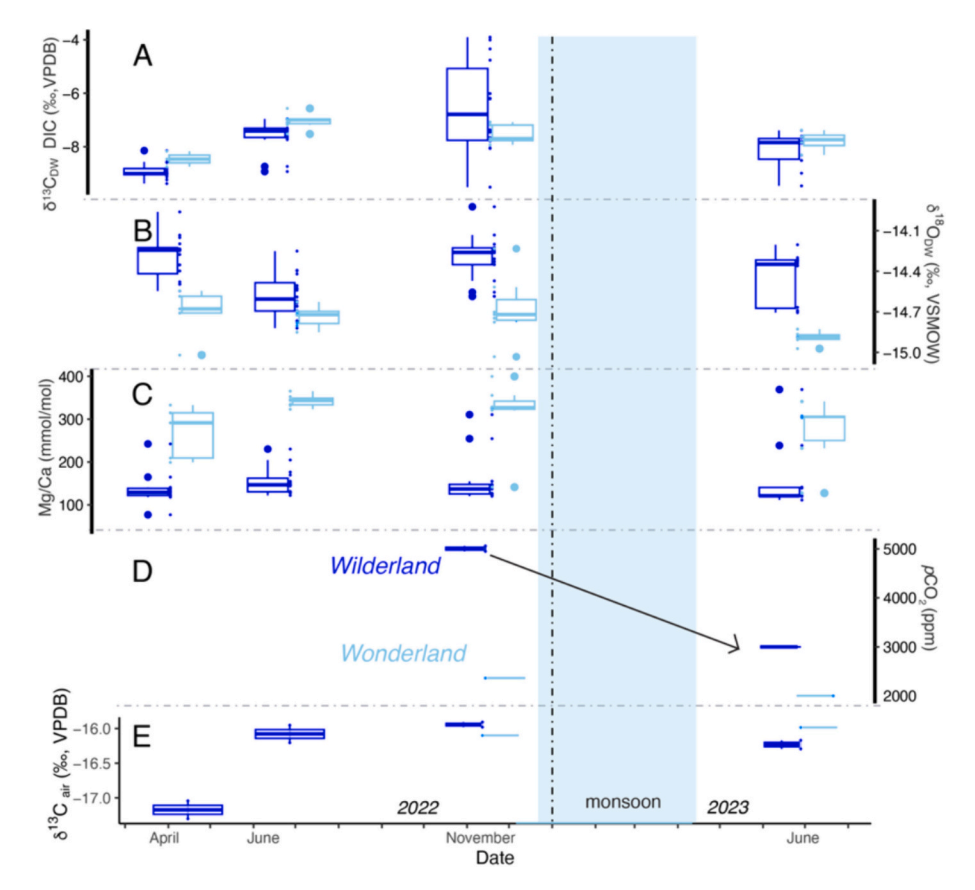


Fig. 6. Intermittent sampling of drip water from the two main study areas in Huagapo. Increased values on all shown variables indicate drying conditions. The highest range in values for all parameters occurs right before the start of the monsoon season in November.

Pacupahuain–Loft had the highest measured calcium concentration of the year (data not shown). The combination of lower pCO_2 and higher calcium concentration in drip rate, therefore, will favor higher calcite precipitation rates during the monsoon and directly after. These factors will combine to produce speleothem calcite records that have a greater amount of calcite from the monsoon season. It is important to note that both Huagapo and Pacupahuain have an increasing pCO_2 gradient from the entrance inward. These pCO_2 gradients will cause the calcite saturation state to depend more on the distance from the entrance rather than seasonal changes. This means that growth rates for Huagapo–Wonderland and Pacupahuain–Aframe will be faster than Huagapo–Wilderland and Pacupahuain–Loft.

Since cave ventilation can profoundly impact the composition of precipitating calcite, many cave monitoring studies focus on the timing of cave ventilation (eg. Borsato et al., 2024; Genty and Deflandre, 1998; Gomell and Pflitsch, 2022). For example, daily cyclic ventilation in Anjohibe Cave in Madagascar was observed by changes in both pCO₂ and RH (Voarintsoa et al., 2021). While in Buraca Gloriosa Cave Portugal, three stochastic ventilation events occurring over a six-year period were recorded by abrupt decreases in RH (Thatcher et al., 2020). In Pacupahuain and Huagapo Caves where we have multiple years of hourly monitoring data, we see no deviations in RH or temperature outside of the sensor accuracy. However, we do see a decrease in the pCO2 of cave air following the monsoon season (2000 ppm difference between seasons; Fig. 6). It is difficult to explain why cave air pCO₂ would decrease during the monsoon as drip rates increase since drip water is the primary source of CO₂ in most caves. However, CO₂ can fluctuate in response to in-cave stream absorption, biological productivity, or even influx from deep-seated thermal geogenic sources. While our measurements were taken with two different methods between November 2022 and June 2023, the measured difference between sampling trips (30–80%) is greater than the reported accuracy of these methods (10%). Therefore, we do not think this decrease is due to analytical techniques. We hypothesize that cave air $\rm CO_2$ drawdown during the wet season may be biologically mediated, though future research should test this. The change in $\rm pCO_2$ combined with our chemistry and sensor data provide evidence for diffuse caveatmospheric exchange rather than rapid ventilation events. Rapid shifts in cave atmosphere can lead to kinetic fractionation effects in calcite and the absence of these events in our caves suggests that this diffuse air exchange is a more favorable ventilation mechanism for incubation of speleothems for paleoclimate records.

5.1.2. Karst Storage and prior calcite precipitation

Karst storage, defined here as the water held for a time in the interconnected fissures, fractures and conduits within a relatively lowpermeability rock matrix, can cause differences in lag time between precipitation events and cave drip water chemistry. Karst terrains with larger storage have greater potential for longer lag times between surface climate conditions and preservation in the speleothem record (Genty et al., 2014; Surić et al., 2018). The drip rate data show an increase during the monsoon (Fig. 3), indicating that there is low karst storage. Drip sensor data show that at diffuse and fracture flow type dominated drip sites waters travel through both primary (pore space) and secondary (fractures) porosity. The fracture dominant flow paths stop during the dry season in the Pacupahuain-Loft Room Syp time series and one drip counter from Huagapo-Wilderland. These drips resumed on February 21st, 2023. Total monsoon rainfall prior to February 21st was 194 mm, which may mark a reservoir threshold. However, it is possible that the threshold for effective recharge is lower due to lag time in flow paths. The reservoir threshold may be as low as 100 mm, the average monthly evapotranspiration rate, which is

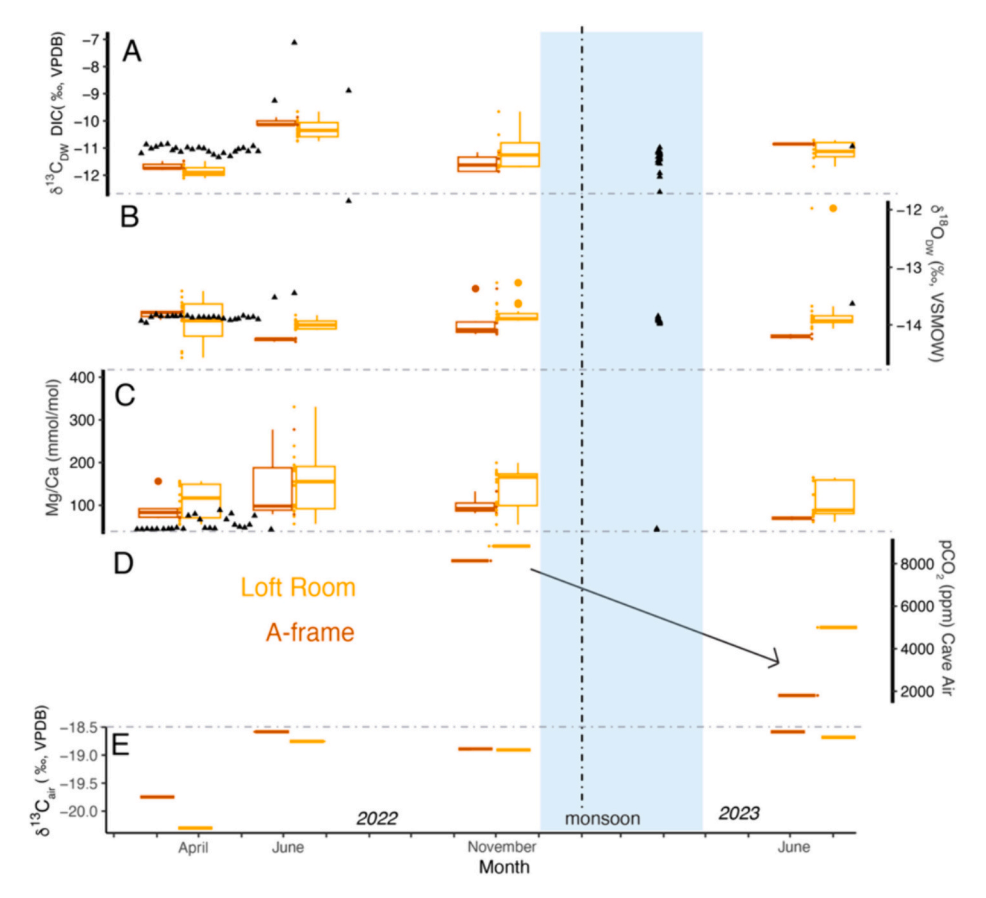


Fig. 7. Intermittent sampling of drip water from the two main study areas (color coded) in Pacupahuain. Continuous Syp autosampler drip waters (black triangles) show the higher dry season peak in Juen and lower monsoon season values in late February. Increased values on all shown variables indicate drying conditions. The highest range in values for all parameters occurs in June–August 2022, but this peak does not repeat in June 2023.

invariable throughout the year in this tropical location (Muñoz et al., 2021). During our November sampling trip, drips were difficult to find. In fact, many attempts to continuously monitor a single drip during this project were thwarted by drips stopping between visits. We attribute this to low karst storage capacity in the system.

Low karst storage is also suggested by the drip water time series and precipitation comparison. The Syp autosampler was located under several fracture-fed drips, and the $\delta^{18}O_{DW}$ values over the year increased from the monsoon to dry seasons. This increase may also be caused by evaporation in the epikarst of monsoon season recharge along flow paths or by infiltration of higher $\delta^{18}O$ precipitation during the dry season. We find the second scenario most likely because the most evaporated $\delta^{18}O_{DW}$ values in the Syp time series occur August 14-17th following an isolated large rain event on August 7th (10.6 mm). Prior to this drip

Table 2Summary of cave carbon isotope values in % VPDB.

Cave Area	Calcite Avg. $\delta^{13}C_c \; (\sigma)$	n	Drip water Avg. $\delta^{13}C_{DW}$ (σ)	n	Cave Air Avg. $\delta^{13}C_{air}$ (σ)	n	Bedrock Avg. $\delta^{13}C_{BR}$ (σ)	n	Soil Avg. $\delta^{13}C_{soil}$ (σ)	n	Vegetation Avg. $\delta^{13}C_{veg}$ (σ)	n
Antipayarguna							-12.8 (0.4)	4	-25.6 (0.1)	2	-25.6 (2.6)	2
Flowstone Room			-9.7 (0.9)	6	_	-			, ,			
Gravel Room	-6.9 (2.7)	5	-10.9 (0.5)	4	-18.9 (0.1)	2						
Huagapo							0.9 (1.5)	6	-25.0 (0.1)	3	-26.6 (1.4)	5
Wilderland	-3.9 (1.8)	10	-7.8 (1.3)	53	-16.4 (0.5)	8						
Wonderland	-5.0 (1.9)	5	-7.5 (0.6)	19	-16.0 (0.1)	2						
Pacupahuain							1.1 (0.2)	3	-25.1 (0.1)	4	-26.6 (2.3)	8
Aframe Room	-3.9 (1.4)	13	-11.2 (0.7)	14	-18.9 (0.5)	4						
Loft Room	-2.8 (1.7)	10	-11.0 (0.8)	89	-19.1 (0.8)	4						

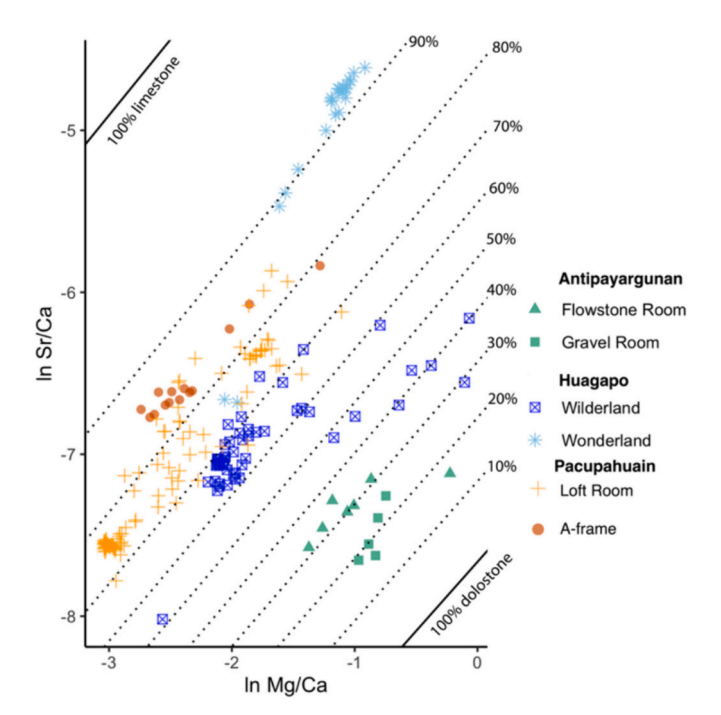


Fig. 8. Trace element ln Sr/Ca and ln Mg/Ca ratios of drip water from all three caves. Dotted lines are the fraction of limestone mixing lines for constant Sr and Mg partition coefficients based on measured cave temperature an equations in (Wassenburg et al., 2020). Samples from each site fall along a fixed mixing ratio line. PCP increases along mixing lines with increased values indicating greater PCP contribution. At Huagapo – Wilderland there is a large range of bedrock mixing proportions from 30 to 60% limestone, with most samples plotting around 55% limestone. All other sites show a much smaller range in the bedrock mixing extent and PCP dominates the observed trends in trace element ratios.

water collection, no drips had occurred for a month, with the previous drip on July 15th. The next rain event, over 10 mm, occurred on November 2nd, but this did not result in drip water in the Syp. Factors such as the rate of rainfall, soil moisture level, and volume of water in epikarst stores could potentially explain why the August event reached the cave while the November event did not. Future work could use dye tracing or radiogenic tracers to determine water residence times and the extent of seasonal drying in the epikarst.

PCP along drying conduits in the epikarst or on stalactites alters the drip water chemistry and the chemical compositions of underlying stalagmites such that they will differ from the original drip water composition along flow paths where PCP is not occurring. Increases in both the calcite carbon and oxygen isotope values are due to PCP, while increases in only carbon are likely due to non-equilibrium degassing of pCO2 during calcite precipitation (Tremaine et al., 2011). In our caves, both $\delta^{13}C_c$ and $\delta^{18}O_c$ increase from the wet to the dry season (Fig. 9). The drip water isotope and trace element data indicate that PCP increases in the dry season. While incongruent bedrock dissolution can create similar dry season increases in trace metals, the isotope data indicate that the process here is PCP. The low karst storage above these caves and the large changes in water balance due to the monsoonal climate likely cause PCP to be a very consistent process. In Golgotha Cave in Australia, low drip rate sites had chemistry indicative of PCP, while fast flow sites did not (Treble et al., 2015). A recent review of cave monitoring studies Lyu et al. (2023) found that in caves with large seasonal differences in rainfall amount and a narrow range of pCO₂, like ours, the degree of PCP reflected in trace element ratios is driven by hydroclimate. We similarly find that PCP is greater during the dry season when drip rates slow and matrix flow dominates throughout the caves.

Previous research has demonstrated that speleothem calcite from

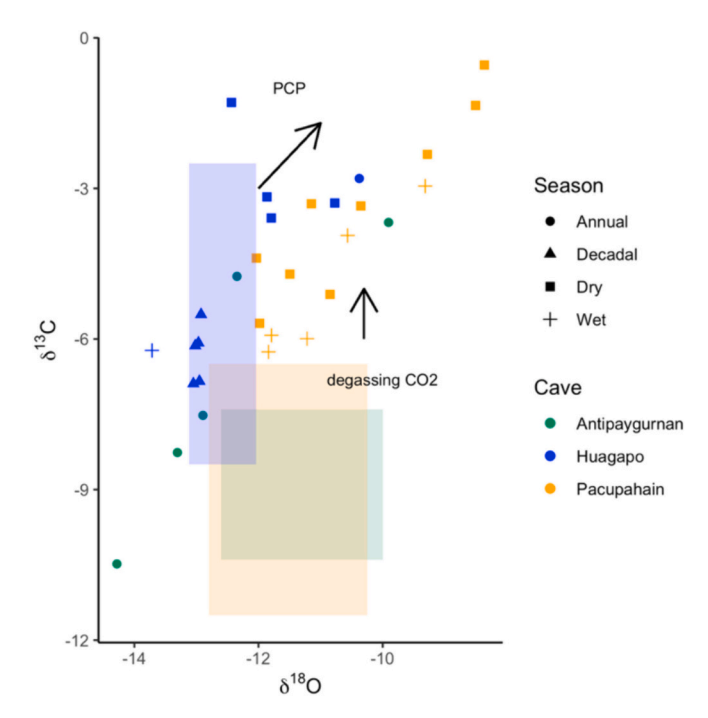


Fig. 9. Isotope values (in ‰) of farmed calcite slides collected over the wet season (cross), dry season(square), and entire year (circle), as well as actively dripping stalagmite tops (triangle). The expected range of equilibrium calcite formation calculated from the ISOLUTION model with values from observed sensor and chemistry data for each cave is plotted in the transparent boxes with colors corresponding to individual caves as per the individual observations. Best fit lines are plotted through the slide data.

Junín area caves record monsoon strength over time (Burns et al., 2019; Burns et al., 2015; Kanner et al., 2013; Kanner et al., 2012), and comparison with Junín lake levels over the Last Glacial Maximum (LGM) confirms this relationship with local hydrologic balance (Woods et al., 2020). Yet, the systematics responsible for preserving this recorded signal had not been investigated. Here, we show that monsoon season precipitation increases drip rate/water in the Junín area caves. This monsoon drip water pulse occurs during a period of relatively lower pCO₂ and leads to higher rates of calcite precipitation. While these waters fill fractures during the monsoon season, their subsequent drainage in the dry season creates a ubiquitous PCP signal in the continued matrix flow. The quick flow paths through fractured bedrock and low karst storage facilitate the pulse of monsoon water occurring and subsequent drying of the system. In this way, the cave environment and karst hydrology facilitate the preservation of the monsoon season in calcite from these caves.

Therefore, the speleothems in the Junín caves record changes in hydrology in their chemistry. This is a bit surprising as previous work by Borsato et al. (2016) demonstrated that along an elevation transect high-altitude cave sites, calcite reflected temperature rather than hydrology, which is recorded in lower elevation caves. This phenomenon occurs because soil pCO $_2$ from vegetation, which drives speleothem growth, is temperature-limited in high alpine environments. In contrast, we find that due to the tropical alpine location of our caves, the drip water seasonality and PCP are controlled by hydrology, not temperature. However, during glacial periods when tropical temperatures are lower, decreased vegetation productivity and soil pCO $_2$ may cause speleothem records from our study region to be temperature-controlled or may prohibit speleothem growth altogether.

5.2. Combing speleothem paleoclimate records from different caves

5.2.1. Mean calcite δ^{18} O and δ^{13} C differences between caves

Speleothem records from wide regional areas are often combined to create composites (e.g., Chen et al., 2016; Meckler et al., 2012). Comparing oxygen isotope values of cave drip water globally, Baker et al. (2019) demonstrated that drip water $\delta^{18}O_{DW}$ values are controlled by differences in mean annual temperature (MAT). At sites where MAT <10 °C drip waters correspond to the annual precipitation amountweighted $\delta^{\bar{18}}O_{precip}$ value and at sites with MAT between 10 and 16 $^{\circ}C$ the recharge-weighted $\delta^{18}O$ value controls drip water $\delta^{18}O_{DW}$. This suggests that within zones of equal MAT, stalagmite records may be combined to create composites. However, difference in kinetic fractionation between drip sites often causes inconsistency among stalagmite records from within the same cave (Stoll et al., 2015). In a global survey of drip water $\delta^{18}O_{DW}$, Treble et al. (2022) found that variability is controlled by flow path and primarily by the degree of fractures along each path length. This suggests, then, that stalagmite selection is critical when creating composite paleoclimate records and that combining records with similar flow path types from different caves within the same climate region may indeed be more logical than the combination of two stalagmites from the same cave that are from different flow path types.

This modern cave monitoring program is the first step toward determining if speleothem records can be combined from multiple caves in the Junín region. By comparing modern cave chemistry, we can anticipate offsets between these cave systems. Drip water $\delta^{18}O_{DW}$ values are offset along the evaporation line between the cave sites (Fig. 5), and this offset is also seen in the calciteo¹⁸O_c values. This suggests that Huagapo and Antipayarguna will have overlapping paleo $\delta^{18}O_c$ values, but contemporaneous Pacupahuain $\delta^{18}O_c$ values will be higher. One potential reason for the higher $\delta^{18}O_{DW}$ values in Pacupahuain is the contribution of shallow groundwater that is more evaporated. The Laguna Gallerina lake provides an analogous sample for long residence time shallow groundwater stores. A simple two-endmember mixing model between mean weighted Huagapo precipitation and Laguna Gallerina lake water estimates that Pacupahuain cave drip waters comprise 41% lake water. The lake water was not sampled during the other times of year, so changes to this end member likely would lower the estimated contribution as lower $\delta^{18}O_{precip}$ monsoon rains are added to the lake over the wet season. The more evaporation-sensitive karst storage above Pacupahuain will cause an $\delta^{18}O_c$ offset between caves and indicates that during very dry periods, stalagmite growth in the cave may cease due to the sensitivity of this system to aridity. To combine the Pacupahuain records with stalagmites from the other caves in the region, we now know that equilibrium offsets as large as 2% in $\delta^{18}O_c$ between caves could occur in the paleorecord due to non-climatic factors. This suggests that normalization of the oxygen isotope value may be the best approach when combining stalagmite records from these caves with large observed offsets.

The drip water in all three caves falls along the local evaporation line, this has previously been observed at arid cave sites (Cuthbert et al., 2014; Duan et al., 2016). Evaporation during infiltration likely causes this offset and informs us that water residence times are reflected in the previously published paleoclimate records from these caves. This finding has important implications for interpreting these records because, during arid periods, similar to today, the water residence time could cause shifts in the $\delta^{18} O_c$ that are due to local hydrologic balance and not changes in the $\delta^{18}\text{O}$ of precipitation. For example, fluid inclusion work in Cueva del Tigre Perdido in the Peruvian Amazon, atmospherically upstream of our study area, shows in that cave drip waters in the Holocene fall on the global meteoric water line and are not evaporated (van Breukelen et al., 2008). During the LGM, there is no shift in the mean $\delta^{18}O_c$ at Cueva del Tigre Perdido, but at Pacupahuain and Huagapo, there is a 3% increase between the glacial and interglacial records. Wang et al. (2017) proposed that moisture recycling facilitated by plant transpiration in the Amazon basin is responsible for the

continental $\delta^{18}O_c$ gradient shifting from 0% to -2.8% over the interglacial-glacial boundary between Cueva Paraiso in the eastern Amazon and Cueva Diamante and Cueva del Tigre Perdido in the western Amazon. Given our findings that drip water today is on average + 1% higher than mean precipitation at the Junín region sites, this difference between glacial and interglacial oxygen isotope gradients may be explained in part by evaporation differences from the interglacial to glacial and not solely moisture recycling. Future work on fluid inclusions from these caves could be done to test if the evaporative signal was present during previous time periods, as has been done at other sites (Bar-Matthews et al., 2003; Fleitmann et al., 2003; Millo et al., 2017).

The value of the actively dripping stalagmite tops measured in Huagapo suggests that the calcite $\delta^{\hat{1}8}O_c$ value will be weighted toward calcite precipitated in isotopic equilibrium, as modeled by ISOLUTION. However, the farmed calcite slides show lower wet season $\delta^{18}O_c$ values and higher dry season values, with the latter plotting outside the modeled equilibrium range in many cases. While PCP can explain some of this range in the $\delta^{18}O_c$ values, it is possible that long water residence times on the flat glass plates, which are not perfectly analogous to curved stalagmite tops, is responsible for the higher measured values. $\delta^{13}C_c$ values of calcite were expected to be offset due to the range in δ¹³C_{DIC} measured. However, differences between the caves are absent in δ¹³C_c of calcite, with overlapping values for all sites. However, in Pacupahuain Cave, there are several measured calcite slides where $\delta^{13}C_c$ values are above the equilibrium value based on drip water and cave conditions. We hypothesize that non-equilibrium degassing of pCO2 occurs in Pacupahuain Cave because of the higher pCO₂ (5000–8000 μatm, Loft Room). Under these very high pCO₂ conditions, calcite precipitation rates will be slow (Dreybrodt and Fohlmeister, 2022) while drip rates are high as the quick change over of the water in the precipitating film will cause disequilibrium between the HCO3 and CO2 (Carlson et al., 2020).

Therefore, we infer that the carbon and oxygen isotope paleoclimate records from these caves will produce similar results for most drip sites. This is due to 1) calcite precipitation rates being highest during the monsoon, 2) ubiquitous PCP in all caves and 3) the higher $\delta^{13}C_c$ values of calcite from Antipayarguna and Pacupahuain Caves due to kinetic effects during non-equilibrium degassing. While isotope trends are similar between flow path types, the trace element drip water data show evidence for flow path mixing between dolomitic limestone host rock compositions.

5.2.2. Trace element concentration differences between cave sites

Trace element concentrations in speleothems are often used as a proxy for precipitation amounts to verify and support isotope interpretations (e.g., Verheyden et al., 2000; Borsato et al., 2007). Applying this proxy assumes that the trace element ratio to calcium concentration will increase if PCP occurs as calcium is preferentially precipitated into the calcite over other trace elements in the water. The inherent assumption is that the trace element composition of the bedrock being dissolved along the flow path does not change. For this reason, trace element concentrations in speleothems are often tested by correlation analysis between Sr/Ca and Mg/Ca ratios, since the slope between these two ratios should remain constant if there is a single source. In our trace element analysis of drip water in each cave (Fig. 8), we found differences in slopes, implying that the host rock trace element composition in the basin was highly variable, suggesting the proportion of dolomitic limestone is variable. Differences in slopes suggest that Wonderland-Huagapo has drip water flow paths through 90% limestone bedrock, whereas waters in Antipayarguna cave are 90% dolostone bedrock hosted. Even though the dolomitic limestone massif is apparently spatially variable, the proportion of limestone-dolostone is consistent at each cave site, except for South Room in Huagapo-Wilderland. Trace element data from the South Room shows a significant range of mixing between bedrock sources with 30 to 60% limestone endmembers for drip waters, suggesting stalagmites from this cave area are not good candidates for trace element-based paleoclimate reconstruction. At all our other cave sites, the trace elements show a consistent evolution along PCP vectors, suggesting that trace element analysis would be useful in these areas for determining if changes in $\delta^{18} O_c$ correspond with changes in precipitation amount.

6. Conclusions

Speleothem proxy records from South America are often inferred to reflect monsoon strength at cave sites throughout the continent. However, the lack of modern cave monitoring in the region prohibits further interpretation of these records, specifically when they are discordant. To aid in the continental-scale interpretation of monsoonal paleoclimate histories, we monitored three important caves in the Peruvian Andes.

While many cave monitoring studies are focused on the assessment of caves and drip sites for future paleoclimate record development, this study has the benefits of previously published paleoclimate records. Rather than asking if the caves are suitable for paleoclimate work, we are asking- what about these caves makes them such good speleothem incubators? We find cave conditions are stable with respect to temperature and relative humidity. The atmospheric pressure data show that cave and outside atmospheric conditions are coupled, signifying that small-scale air exchange likely occurs on a diurnal scale but has little to no impact on the cave environment (i.e., temperature and RH). Seasonal drip water chemistry changes over the year with monsoon fracture flow contribution, and PCP occurring throughout the caves in the dry season. The isotopic composition of drip waters falls along the local evaporation line, so evaporation in the unsaturated zone alters the initial rainfall composition. These findings in an exploratory cave study could be used to suggest that these caves would not be good candidates for paleoclimate work. However, given past publications showing the exceptional correlation among stalagmites from these caves and extratropical and regional climate forcings, we hypothesize that the large drip water pulse during the monsoon dominates many of these records. This is supported by our finding that the isotope values in the modern stalagmite tops fall within the equilibrium modeled range. This monsoonal weighting of cave calcite occurs because of low karst storage and high calcite precipitation rates during wet conditions. In this way, the cave processes amplify the monsoon signal, preserving this hydrologic response in the speleothem records. These records are, therefore, highly seasonal, and comparison with other paleo-records may provide information on changing seasonality over time.

Proxy offsets between the cave sites include differences in oxygen/carbon isotopes and trace element concentrations. The calcite and drip water isotope values for Huagapo differ slightly from those for Pacupahuain and Antipayarguna caves. The combination of isotope records from the caves should consider that offsets may exist and should be considered for overlapping stalagmite records from different caves. Specifically, our data show that Pacupahuain Cave is expected to have higher carbon and oxygen isotope values than Huagapo Cave. The observed range provides a baseline for contemporaneous offsets in paleo-records from these caves. The offset in trace elements is likely due to the variable flow paths through different host rocks. The combination of trace element data must account for these different host rock baselines. Given the wide range of bedrock values, future trace metal work will likely need to normalize data to compare individual speleothems and certainly between the different caves.

While our study has multiple years of monitoring data from the caves. Future work could improve our understanding of paleoclimate records by monitoring drip water geochemistry over multiple years. However, after monsoon intensity, the El Niño Sothern Oscillation is the main source of local variability in the δ^{18} O_{precip} of precipitation in the region (Thompson et al., 2017; Thompson et al., 2013; Vuille and Werner, 2005). Future work should contain at least a few ENSO cycles of data to address cave conditional response to these drivers of atmospheric

variability. Alternatively, high-resolution work on a modern growing speleothem could address questions concerning inter-annual variations. Monitoring of the Antipayarguna Cave was minimal (wet versus dry season), and further monitoring would improve the interpretation of records from it.

This study improves the interpretation of speleothem records from High Andean caves by determining the seasonality of calcite precipitation rates and the offsets between cave sites, which may persist in the paleorecord. Future work will apply these findings to the paleoclimatic record from the region.

CRediT authorship contribution statement

Elizabeth Olson: Writing – review & editing, Writing – original draft, Visualization, Validation, Project administration, Methodology, Investigation, Formal analysis, Data curation, Conceptualization. David P. Gillikin: Writing - review & editing, Writing - original draft, Supervision, Resources, Project administration, Methodology, Investigation, Funding acquisition, Conceptualization. Laura Piccirillo: Methodology, Investigation, Formal analysis, Data curation. Anouk Verheyden: Methodology, Formal analysis, Data curation. Alexander Forsyth: Investigation, Formal analysis, Data curation. Kirsten Litchfield: Investigation, Formal analysis. Hailey Stoltenberg: Investigation, Formal analysis. Avery Clavel: Investigation, Formal analysis. Maryam Ramjohn: Investigation, Formal analysis. Saliha Nazir: Investigation, Formal analysis. Pedro M. Tapia: Resources, Project administration, Investigation. Dylan Parmenter: Investigation. Donald T. Rodbell: Writing - review & editing, Writing - original draft, Resources, Project administration, Methodology, Investigation, Funding acquisition, Conceptualization.

Declaration of competing interest

The authors declare the following financial interests/personal relationships which may be considered as potential competing interests.

Donald Rodbell reports financial support was provided by National Science Foundation. David Gillikin reports was provided by National Science Foundation. If there are other authors, they declare that they have no known competing financial interests or personal relationships that could have appeared to influence the work reported in this paper.

Data availability

The data for this article is provided in the supplemental data tables provided. All code for figures shown can be made available upon request.

Acknowledgements

We are grateful for the precipitation collection volunteers, Esequel Chuquivilca and Ramiro Castro. Thanks to Guiro Yurivilca Vega for access and guidance through Pacupahuain Cave. We thank Sophie Verheyden and Diana Thatcher for helpful discussions about this study. This work was supported by the U.S. National Science Foundation (NSF-EAR 2102996) to D.T.R. and D.P.G, as well as Union College Funding. D. P. was funded via NSF (EAR 2103020). The U.S. National Science Foundation funded Union College's isotope ratio mass spectrometer and peripherals (NSF-MRI #1229258), the Picarro CRDS (NSF-MRI #2018836), and the ICP-MS (NSF-MRI # 1726075).

Appendix A. Supplementary data

Supplementary data to this article can be found online at https://doi. org/10.1016/j.chemgeo.2024.122315.

References

- Baker, A., Smith, C., Jex, C., Fairchild, I., Genty, D., Fuller, L., 2008. Annually laminated speleothems: a review. IJS 37, 193–206. https://doi.org/10.5038/1827-806X.37.3.4.
- Baker, A., Hartmann, A., Duan, W., Hankin, S., Comas-Bru, L., Cuthbert, M.O., Treble, P. C., Banner, J., Genty, D., Baldini, L.M., Bartolomé, M., Moreno, A., Pérez-Mejías, C., Werner, M., 2019. Global analysis reveals climatic controls on the oxygen isotope composition of cave drip water. Nat. Commun. 10, 2984. https://doi.org/10.1038/s41467-019-11027-w.
- Bar-Matthews, M., Ayalon, A., Kaufman, A., Wasserburg, G.J., 1999. The Eastern Mediterranean paleoclimate as a reflection of regional events: Soreq cave, Israel. Earth Planet. Sci. Lett. 166, 85–95. https://doi.org/10.1016/S0012-821X(98)00275-
- Bar-Matthews, M., Ayalon, A., Gilmour, M., Matthews, A., Hawkesworth, C.J., 2003. Sea-land oxygen isotopic relationships from planktonic foraminifera and speleothems in the Eastern Mediterranean region and their implication for paleorainfall during interglacial intervals. Geochim. Cosmochim. Acta 67, 3181–3199. https://doi.org/10.1016/S0016-7037(02)01031-1.
- Bernal, J.P., Revolorio, F., Cu-Xi, M., Lases-Hernández, F., Piacsek, P., Lachniet, M.S., Beddows, P.A., Lucia, G., López-Aguiar, K., Capella-Vizcaíno, S., López-Martínez, R., Vásquez, O.J., 2023. Variability of trace-elements and 8180 in drip water from Gruta del Rey Marcos, Guatemala; seasonal and environmental effects, and its implications for paleoclimate reconstructions. Front. Earth Sci. 11, 1112957. https://doi.org/ 10.3389/feart.2023.1112957.
- Borsato, A., Frisia, S., Fairchild, I.J., Somogyi, A., Susini, J., 2007. Trace element distribution in annual stalagmite laminae mapped by micrometer-resolution X-ray fluorescence: Implications for incorporation of environmentally significant species. Geochim. Cosmochim. Acta 71, 1494–1512. https://doi.org/10.1016/j. gca.2006.12.016.
- Borsato, A., Johnston, V.E., Frisia, S., Miorandi, R., Corradini, F., 2016. Temperature and altitudinal influence on karst dripwater chemistry: Implications for regional-scale palaeoclimate reconstructions from speleothems. Geochim. Cosmochim. Acta 177, 275–297. https://doi.org/10.1016/i.gca.2015.11.043.
- 275–297. https://doi.org/10.1016/j.gca.2015.11.043.
 Borsato, A., Samadelli, M., Martimucci, V., Manzi, G., 2024. Temperature fluctuations and ventilation dynamics induced by atmospheric pressure variations in Lamalunga Cave (Apulia, Italy) and their influences on speleothem growth. Quat. Res. 118, 100–115. https://doi.org/10.1017/qua.2023.70.
- Bouillon, S., Yambélé, A., Gillikin, D.P., Teodoru, C., Darchambeau, F., Lambert, T., Borges, A.V., 2014. Contrasting biogeochemical characteristics of the Oubangui River and tributaries (Congo River basin). Sci. Rep. 4, 5402. https://doi.org/ 10.1038/srep05402.
- Bouillon, S., Yambélé, A., Spencer, R.G.M., Gillikin, D.P., Hernes, P.J., Six, J., Merckx, R., Borges, A.V., 2012. Organic matter sources, fluxes and greenhouse gas exchange in the Oubangui River (Congo River basin). Biogeosciences 9, 2045–2062. https://doi. org/10.5194/bs-0-2045-2012
- Breecker, D.O., 2017. Atmospheric pCO 2 control on speleothem stable carbon isotope compositions. Earth Planet. Sci. Lett. 458, 58–68. https://doi.org/10.1016/j. epsl 2016 10.042
- Bühler, J.C., Axelsson, J., Lechleitner, F.A., Fohlmeister, J., LeGrande, A.N., Midhun, M., Sjolte, J., Werner, M., Yoshimura, K., Rehfeld, K., 2022. Investigating stable oxygen and carbon isotopic variability in speleothem records over the last millennium using multiple isotope-enabled climate models. Clim. Past 18, 1625–1654. https://doi. org/10.5194/cp-18-1625-2022.
- Burns, S.J., Kanner, L.C., Cheng, H., Lawrence Edwards, R., 2015. A tropical speleothem record of glacial inception, the South American Summer Monsoon from 125 to 115 ka. Clim. Past 11, 931–938. https://doi.org/10.5194/cp-11-931-2015.
- Burns, S.J., Welsh, L.K., Scroxton, N., Cheng, H., Edwards, R.L., 2019. Millennial and orbital scale variability of the South American Monsoon during the penultimate glacial period. Sci. Rep. 9, 1234. https://doi.org/10.1038/s41598-018-37854-3.
- Campos, J.L.P.S., Cruz, F.W., Ambrizzi, T., Deininger, M., Vuille, M., Novello, V.F., Strikis, N.M., 2019. Coherent South American Monsoon Variability during the last Millennium Revealed through High-Resolution Proxy Records. Geophys. Res. Lett. 46, 8261–8270. https://doi.org/10.1029/2019GL082513.
- Carlson, P.E., Noronha, A.L., Banner, J.L., Jenson, J.W., Moore, M.W., Partin, J.W., Deininger, M., Breecker, D.O., Bautista, K.K., 2020. Constraining speleothem oxygen isotope disequilibrium driven by rapid CO2 degassing and calcite precipitation: Insights from monitoring and modeling. Geochim. Cosmochim. Acta 284, 222–238. https://doi.org/10.1016/j.gca.2020.06.012.
- Chen, S., Wang, Y., Cheng, H., Edwards, R.L., Wang, X., Kong, X., Liu, D., 2016. Strong coupling of Asian Monsoon and Antarctic climates on sub-orbital timescales. Sci. Rep. 6, 32995. https://doi.org/10.1038/srep32995.
- Cobb, K.M., Adkins, J.F., Partin, J.W., Clark, B., 2007. Regional-scale climate influences on temporal variations of rainwater and cave dripwater oxygen isotopes in northern Borneo. Earth Planet. Sci. Lett. 263, 207–220. https://doi.org/10.1016/j. cop/ 2007.08.024
- Comas-Bru, L., Rehfeld, K., Roesch, C., Amirnezhad-Mozhdehi, S., Harrison, S.P., Atsawawaranunt, K., Ahmad, S.M., Brahim, Y.A., Baker, A., Bosomworth, M., Breitenbach, S.F.M., Burstyn, Y., Columbu, A., Deininger, M., Demény, A., Dixon, B., Fohlmeister, J., Hatvani, I.G., Hu, J., Kaushal, N., Kern, Z., Labuhn, I., Lechleitner, F. A., Lorrey, A., Martrat, B., Novello, V.F., Oster, J., Pérez-Mejías, C., Scholz, D., Scroxton, N., Sinha, N., Ward, B.M., Warken, S., Zhang, H., SISAL Working Group members, 2020. SISALv2: a comprehensive speleothem isotope database with multiple age-depth models. Earth Syst. Sci. Data 12, 2579–2606. https://doi.org/10.5194/essd-12-2579-2020.

- Cruz, F.W., Karmann, I., Viana, O., Burns, S.J., Ferrari, J.A., Vuille, M., Sial, A.N., Moreira, M.Z., 2005. Stable isotope study of cave percolation waters in subtropical Brazil: Implications for paleoclimate inferences from speleothems. Chem. Geol. 220, 245–262. https://doi.org/10.1016/j.chemgeo.2005.04.001.
- Cruz, F.W., Vuille, M., Burns, S.J., Wang, X., Cheng, H., Werner, M., Lawrence Edwards, R., Karmann, I., Auler, A.S., Nguyen, H., 2009. Orbitally driven east—west antiphasing of south American precipitation. Nat. Geosci. 2, 210–214. https://doi. org/10.1038/ngeo444.
- Cuthbert, M.O., Baker, A., Jex, C.N., Graham, P.W., Treble, P.C., Andersen, M.S., Ian Acworth, R., 2014. Drip water isotopes in semi-arid karst: Implications for speleothem paleoclimatology. Earth Planet. Sci. Lett. 395, 194–204. https://doi.org/ 10.1016/j.epsl.2014.03.034.
- Deininger, M., Ward, B.M., Novello, V.F., Cruz, F.W., 2019. Late Quaternary Variations in the South American Monsoon System as Inferred by Speleothems—New Perspectives using the SISAL Database. Quaternary 2, 6. https://doi.org/10.3390/ guat/2010006
- Domínguez-Villar, D., Krklec, K., Sierro, F.J., 2023. Thermal conduction in karst terrains dominating cave atmosphere temperatures: Quantification of thermal diffusivity. Int. J. Therm. Sci. 189, 108282. https://doi.org/10.1016/j.ijthermalsci.2023.108282.
- Dreybrodt, W., Fohlmeister, J., 2022. The impact of outgassing of CO2 and prior calcium precipitation to the isotope composition of calcite precipitated on stalagmites. Implications for reconstructing climate information from proxies. Chem. Geol. 589, 120676. https://doi.org/10.1016/j.chemgeo.2021.120676.
- Duan, W., Ruan, J., Luo, W., Li, T., Tian, L., Zeng, G., Zhang, D., Bai, Y., Li, J., Tao, T., Zhang, P., Baker, A., Tan, M., 2016. The transfer of seasonal isotopic variability between precipitation and drip water at eight caves in the monsoon regions of China. Geochim. Cosmochim. Acta 183, 250–266. https://doi.org/10.1016/j.gca.2016.03.037.
- Duan, P., Li, H., Sinha, A., Voarintsoa, N.R.G., Kathayat, G., Hu, P., Zhang, H., Ning, Y., Cheng, H., 2021. The timing and structure of the 8.2 ka event revealed through highresolution speleothem records from northwestern Madagascar. Quat. Sci. Rev. 268, 107104. https://doi.org/10.1016/j.quascirev.2021.107104.
- Fairchild, I.J., Baker, A., 2012. Speleothem Science: From Process to Past Environments. John Wiley & Sons.
- Fairchild, I.J., Borsato, A., Tooth, A.F., Frisia, S., Hawkesworth, C.J., Huang, Y., McDermott, F., Spiro, B., 2000. Controls on Trace Element žSr–mg/ Compositions of Carbonate Cave Waters: Implications for Speleothem Climatic Records.
- Fairchild, I.J., Smith, C.L., Baker, A., Fuller, L., Spötl, C., Mattey, D., McDermott, F., E.I. M.F, 2006. Modification and preservation of environmental signals in speleothems. Earth Sci. Rev. 75, 105–153. https://doi.org/10.1016/j.earscirev.2005.08.003.
- Fleitmann, D., Burns, S.J., Neff, U., Mangini, A., Matter, A., 2003. Changing moisture sources over the last 330,000 years in Northern Oman from fluid-inclusion evidence in speleothems. Quat. Res. 60, 223–232. https://doi.org/10.1016/S0033-5894(03) 00086-3
- Fohlmeister, J., Voarintsoa, N.R.G., Lechleitner, F.A., Boyd, M., Brandtstätter, S., Jacobson, M.J., Oster, L.J., 2020. Main controls on the stable carbon isotope composition of speleothems. Geochim. Cosmochim. Acta 279, 67–87. https://doi. org/10.1016/j.gca.2020.03.042.
- Garreaud, R., Vuille, M., Clement, A.C., 2003. The climate of the Altiplano: observed current conditions and mechanisms of past changes. Palaeogeogr. Palaeoclimatol. Palaeoecol. 194, 5–22. https://doi.org/10.1016/S0031-0182(03)00269-4.
- Genty, D., Deflandre, G., 1998. Drip flow variations under a stalactite of the Pere Noel cave (Belgium). Evidence of seasonal variations and air pressure constraints. J. Hydrol. 211, 208–232.
- Genty, D., Labuhn, I., Hoffmann, G., Danis, P.A., Mestre, O., Bourges, F., Wainer, K., Massault, M., Van Exter, S., Régnier, E., Orengo, Ph., Falourd, S., Minster, B., 2014. Rainfall and cave water isotopic relationships in two South-France sites. Geochim. Cosmochim. Acta 131, 323–343. https://doi.org/10.1016/j.gca.2014.01.043.
- Gillikin, D.P., Bouillon, S., 2007. Determination of δ18O of water and δ13C of dissolved inorganic carbon using a simple modification of an elemental analyser-isotope ratio mass spectrometer: an evaluation. Rapid Communicat. Mass Spectrometr. 21, 1475–1478
- Gomell, A.K., Pflitsch, A., 2022. Airflow dynamics in Wind Cave and Jewel Cave: how do barometric caves breathe? IJS 51, 163–179. https://doi.org/10.5038/1827-2068/51.3.2427
- Graniero, L.E., Gillikin, D.P., Surge, D., 2021. Evaluating Freshwater Mussel Shell δ^{13} C Values as a Proxy for Dissolved Inorganic Carbon δ^{13} C Values in a Temperate River. JGR Biogeosci. 126 https://doi.org/10.1029/2020JG006003 e2020JG006003.
- Hardt, B., Rowe, H.D., Springer, G.S., Cheng, H., Edwards, R.L., 2010. The seasonality of east central north American precipitation based on three coeval Holocene speleothems from southern West Virginia. Earth Planet. Sci. Lett. 295, 342–348. https://doi.org/10.1016/j.epsl.2010.04.002.
- INGEMMET, 2017. Mapa Geologico generalizado-Proyecto GE34A-3 "Prospección de Recursos de Rocas y Minerales Industriales de la Región Junín. Republica de Peru, Lima, Peru.
- James, E.W., Banner, J.L., Hardt, B., 2015. A global model for cave ventilation and seasonal bias in speleothem paleoclimate records. Geochem. Geophys. Geosyst. 16, 1044–1051. https://doi.org/10.1002/2014GC005658.
- Jaqueto, P., Trindade, R.I.F., Hartmann, G.A., Novello, V.F., Cruz, F.W., Karmann, I., Strauss, B.E., Feinberg, J.M., 2016. Linking speleothem and soil magnetism in the Pau d'Alho cave (Central South America). JGR Solid Earth 121, 7024–7039. https://doi.org/10.1002/2016JB013541.
- Kanner, L.C., Burns, S.J., Cheng, H., Edwards, R.L., 2012. High-Latitude Forcing of the South American Summer Monsoon during the last Glacial. Science 335, 570–573. https://doi.org/10.1126/science.1213397.

Kanner, L.C., Burns, S.J., Cheng, H., Edwards, R.L., Vuille, M., 2013. High-resolution variability of the south American summer monsoon over the last seven millennia: insights from a speleothem record from the central Peruvian Andes. Quat. Sci. Rev. 75, 1–10. https://doi.org/10.1016/j.quascirev.2013.05.008.

- Kelemen, Z., Gillikin, D.P., Graniero, L.E., Havel, H., Darchambeau, F., Borges, A.V., Yambélé, A., Bassirou, A., Bouillon, S., 2017. Calibration of hydroclimate proxies in freshwater bivalve shells from Central and West Africa. Geochim. Cosmochim. Acta 208, 41–62. https://doi.org/10.1016/j.gca.2017.03.025.
- Lachniet, M.S., Bernal, J.P., Asmerom, Y., Polyak, V., Piperno, D., 2012. A 2400 yr Mesoamerican rainfall reconstruction links climate and cultural change. Geology 40, 259–262. https://doi.org/10.1130/G32471.1.
- Lases-Hernandez, F., Medina-Elizalde, M., Burns, S., DeCesare, M., 2019. Long-term monitoring of drip water and groundwater stable isotopic variability in the Yucatán Peninsula: Implications for recharge and speleothem rainfall reconstruction. Geochim. Cosmochim. Acta 246, 41–59. https://doi.org/10.1016/j. gca.2018.11.028.
- Li, Y., Rao, Z., Xu, Q., Zhang, S., Liu, X., Wang, Z., Cheng, H., Edwards, R.L., Chen, F., 2020. Inter-relationship and environmental significance of stalagmite δ13C and δ18O records from Zhenzhu Cave, North China, over the last 130 ka. Earth Planet. Sci. Lett. 536, 116149. https://doi.org/10.1016/j.epsl.2020.116149.
- Li, Y., Yang, Yan, Jiang, X., Zhao, J., Sun, Z., Shi, X., Tian, N., Yang, Yunyue, Li, J., Duan, J., 2021. The transport mechanism of carbon isotopes based on 10 years of cave monitoring: Implications for paleoclimate reconstruction. J. Hydrol. 592, 125841. https://doi.org/10.1016/j.jhydrol.2020.125841.
- Liu, X., Liu, J., Shen, C.-C., Yang, Y., Chen, J., Chen, S., Wang, X., Wu, C.-C., Chen, F., 2020. Inconsistency between records of δ ¹⁸ O and trace element ratios from stalagmites: evidence for increasing mid–late Holocene moisture in arid Central Asia. The Holocene 30, 369–379. https://doi.org/10.1177/0959683619887431.
- Lyu, Y., Luo, W., Wang, Y., Zeng, G., Chen, J., Wang, S., 2023. Response of drip water Mg/ca and Sr/ca variations in ventilated caves to hydroclimate. Sci. Total Environ. 874, 162626. https://doi.org/10.1016/j.scitotenv.2023.162626.
- Meckler, A.N., Clarkson, M.O., Cobb, K.M., Sodemann, H., Adkins, J.F., 2012. Interglacial Hydroclimate in the Tropical West Pacific through the late Pleistocene. Science 336, 1301–1304. https://doi.org/10.1126/science.1218340.
- Millo, C., Strikis, N.M., Vonhof, H.B., Deininger, M., Da Cruz, F.W., Wang, X., Cheng, H., Lawrence Edwards, R., 2017. Last glacial and Holocene stable isotope record of fossil dripwater from subtropical Brazil based on analysis of fluid inclusions in stalagmites. Chem. Geol. 468, 84–96. https://doi.org/10.1016/j.chemgeo.2017.08.018.
- Muñoz, R., Huggel, C., Drenkhan, F., Vis, M., Viviroli, D., 2021. Comparing model complexity for glacio-hydrological simulation in the data-scarce Peruvian Andes. Journal of Hydrology: Regional Studies 37, 100932. https://doi.org/10.1016/j. airb.2021.10032.
- Orrison, R., Vuille, M., Smerdon, J.E., Apaéstegui, J., Azevedo, V., Campos, J.L.P.S., Cruz, F.W., Della Libera, M.E., Stríkis, N.M., 2022. South American Summer Monsoon variability over the last millennium in paleoclimate records and isotopeenabled climate models. Clim. Past 18, 2045–2062. https://doi.org/10.5194/cp-18-2045-2062.
- Oster, J.L., Montañez, I.P., Kelley, N.P., 2012. Response of a modern cave system to large seasonal precipitation variability. Geochim. Cosmochim. Acta 91, 92–108. https:// doi.org/10.1016/j.gca.2012.05.027.
- Powell, R.L., Yoo, E.-H., Still, C.J., 2012. Vegetation and soil carbon-13 isoscapes for South America: integrating remote sensing and ecosystem isotope measurements. Ecosphere 3, 1–25. https://doi.org/10.1890/ES12-00162.1.
- Pracný, P., Faimon, J., Všianský, D., Přichystal, A., 2019. Evolution of Mg/ca and Sr/ca ratios during the experimental dissolution of limestone. Chem. Geol. 523, 107–120. https://doi.org/10.1016/j.chemgeo.2019.05.040.
- Sammartino, Y., Staccioli, G., Klein, J.D., 1980. Pérou 79 : Le karst de Palcamayo. Bulletin du Groupe Spéléologique Bagnols Marcoule 8, 90–113.
- Sekhon, N., Novello, V.F., Cruz, F.W., Wortham, B.E., Ribeiro, T.G.R., Breecker, D.O., 2021. Diurnal to seasonal ventilation in Brazilian caves. Glob. Planet. Chang. 197, 103378. https://doi.org/10.1016/j.gloplacha.2020.103378.
- Serrato Marks, G., Medina-Elizalde, M., Burns, S., Weldeab, S., Lases-Hernandez, F., Cazares, G., McGee, D., 2021. Evidence for Decreased Precipitation Variability in the Yucatán Peninsula during the Mid-Holocene. Paleoceanog. Paleoclimatol. 36 https://doi.org/10.1029/2021PA004219 e2021PA004219.
- Smart, P.L., Friedrich, H., 1987. Water movement and storage in the unsaturated zone of a matuerly karstified aquifer, Mendip Hills, England. In: Proceedings. Presented at the Conference on Environmental Problems in Karst Terrains and Their Solutions. National Water Well Association, Bowling Green, Kentucky, pp. 57–87.
- Stoll, H., Mendez-Vicente, A., Gonzalez-Lemos, S., Moreno, A., Cacho, I., Cheng, H., Edwards, R.L., 2015. Interpretation of orbital scale variability in mid-latitude speleothem δ18O: significance of growth rate controlled kinetic fractionation effects. Quat. Sci. Rev. 127, 215–228. https://doi.org/10.1016/j.quascirev.2015.08.025.
- Surić, M., Lončarić, R., Bočić, N., Lončar, N., Buzjak, N., 2018. Monitoring of selected caves as a prerequisite for the speleothem-based reconstruction of the Quaternary environment in Croatia. Quat. Int. 494, 263–274. https://doi.org/10.1016/j.quaint.2017.06.042.
- Thatcher, D.L., Wanamaker, A.D., Denniston, R.F., Ummenhofer, C.C., Regala, F.T., Jorge, N., Haws, J., Chormann, A., Gillikin, D.P., 2020. Linking the karst record to atmospheric, precipitation, and vegetation dynamics in Portugal. Chem. Geol. 558, 119949. https://doi.org/10.1016/j.chemgeo.2020.119949.
- Thermo Finnigan, 2004. Thermo Finnigan GasBench II Operating Manual Revision.
- Thompson, L.G., Mosley-Thompson, E., Davis, M.E., Zagorodnov, V.S., Howat, I.M., Mikhalenko, V.N., Lin, P.-N., 2013. Annually Resolved Ice Core Records of Tropical

- Climate Variability over the past \sim 1800 years. Science 340, 945–950. https://doi.org/10.1126/science.1234210.
- Thompson, L.G., Davis, M.E., Mosley-Thompson, E., Beaudon, E., Porter, S.E., Kutuzov, S., Lin, P.-N., Mikhalenko, V.N., Mountain, K.R., 2017. Impacts of recent Warming and the 2015/2016 El Niño on Tropical Peruvian Ice Fields. JGR-Atmos. 122 https://doi.org/10.1002/2017JD026592.
- Treble, P.C., Fairchild, I.J., Griffiths, A., Baker, A., Meredith, K.T., Wood, A., McGuire, E., 2015. Impacts of cave air ventilation and in-cave prior calcite precipitation on Golgotha Cave dripwater chemistry, Southwest Australia. Quat. Sci. Rev. 127, 61–72. https://doi.org/10.1016/j.quascirev.2015.06.001.
- Treble, P.C., Baker, A., Abram, N.J., Hellstrom, J.C., Crawford, J., Gagan, M.K., Borsato, A., Griffiths, A.D., Bajo, P., Markowska, M., Priestley, S.C., Hankin, S., Paterson, D., 2022. Ubiquitous karst hydrological control on speleothem oxygen isotope variability in a global study. Commun. Earth Environ. 3, 29. https://doi.org/10.1038/s43247-022-00347-3.
- Tremaine, D.M., Froelich, P.N., 2013. Speleothem trace element signatures: a hydrologic geochemical study of modern cave dripwaters and farmed calcite. Geochim. Cosmochim. Acta 121, 522–545. https://doi.org/10.1016/j.gca.2013.07.026.
- Tremaine, D.M., Froelich, P.N., Wang, Y., 2011. Speleothem calcite farmed in situ: Modern calibration of δ18O and δ13C paleoclimate proxies in a continuously-monitored natural cave system. Geochim. Cosmochim. Acta 75, 4929–4950. https://doi.org/10.1016/j.gca.2011.06.005.
- Vaks, A., Bar-Matthews, M., Ayalon, A., Schilman, B., Gilmour, M., Hawkesworth, C.J., Frumkin, A., Kaufman, A., Matthews, A., 2003. Paleoclimate reconstruction based on the timing of speleothem growth and oxygen and carbon isotope composition in a cave located in the rain shadow in Israel. Quat. Res. 59, 182–193. https://doi.org/10.1016/\$0033-5894(03)00013-9.
- van Breukelen, M.R., Vonhof, H.B., Hellstrom, J.C., Wester, W.C.G., Kroon, D., 2008. Fossil dripwater in stalagmites reveals Holocene temperature and rainfall variation in Amazonia. Earth Planet. Sci. Lett. 275, 54–60. https://doi.org/10.1016/j. epsl.2008.07.060.
- Voarintsoa, N.R.G., Therre, S., 2022. Using the triple proxy \u03b313C-radiocarbon-major and trace elements to understand stalagmite stable carbon composition in Madagascar. Chem. Geol. 608, 121044. https://doi.org/10.1016/j.chemgeo.2022.121044.
- Verheyden, S., Keppens, E., Fairchild, I.J., McDermott, F., Weis, D., 2000. Mg, Sr and Sr isotope geochemistry of a Belgian Holocene speleothem: implications for paleoclimate reconstructions. Chemical Geology 169, 131–144. https://doi.org/10.1016/S0009-2541(00)00299-0.
- Voarintsoa, N.R.G., Ratovonanahary, A.L.J., Rakotovao, A.Z.M., Bouillon, S., 2021. Understanding the linkage between regional climatology and cave geochemical parameters to calibrate speleothem proxies in Madagascar. Sci. Total Environ. 784, 147181. https://doi.org/10.1016/j.scitotenv.2021.147181.
- Vuille, M., Werner, M., 2005. Stable isotopes in precipitation recording south American summer monsoon and ENSO variability: observations and model results. Clim. Dyn. 25, 401–413. https://doi.org/10.1007/s00382-005-0049-9.
- Wang, X., Edwards, R.L., Auler, A.S., Cheng, H., Kong, X., Wang, Y., Cruz, F.W., Dorale, J. A., Chiang, H.-W., 2017. Hydroclimate changes across the Amazon lowlands over the past 45,000 years. Nature 541, 204–207. https://doi.org/10.1038/nature20787.
- Ward, B.M., Wong, C.I., Novello, V.F., McGee, D., Santos, R.V., Silva, L.C.R., Cruz, F.W., Wang, X., Edwards, R.L., Cheng, H., 2019. Reconstruction of Holocene coupling between the South American Monsoon System and local moisture variability from speleothem δ18O and 87Sr/86Sr records. Quaternary Science Reviews 210, 51–63. https://doi.org/10.1016/j.quascirev.2019.02.019.
- Wassenburg, J.A., Riechelmann, S., Schröder-Ritzrau, A., Riechelmann, D.F.C., Richter, D.K., Immenhauser, A., Terente, M., Constantin, S., Hachenberg, A., Hansen, M., Scholz, D., 2020. Calcite Mg and Sr partition coefficients in cave environments: Implications for interpreting prior calcite precipitation in speleothems. Geochim. Cosmochim. Acta 269, 581–596. https://doi.org/10.1016/j. gca.2019.11.011.
- Wolf, A., Roberts, W.H.G., Ersek, V., Johnson, K.R., Griffiths, M.L., 2020. Rainwater isotopes in Central Vietnam controlled by two oceanic moisture sources and rainout effects. Sci. Rep. 10, 16482. https://doi.org/10.1038/s41598-020-73508-z.
- Woods, A., Rodbell, D.T., Abbott, M.B., Hatfield, R.G., Chen, C.Y., Lehmann, S.B., McGee, D., Weidhaas, N.C., Tapia, P.M., Valero-Garcés, B.L., Bush, M.B., Stoner, J.S., 2020. Andean drought and glacial retreat tied to Greenland warming during the last glacial period. Nat Commun 11, 5135. https://doi.org/10.1038/s41467-020-19000-8
- Wortham, B.E., Wong, C.I., Silva, L.C.R., McGee, D., Montañez, I.P., Troy Rasbury, E., Cooper, K.M., Sharp, W.D., Glessner, J.J.G., Santos, R.V., 2017. Assessing response of local moisture conditions in Central Brazil to variability in regional monsoon intensity using speleothem 87Sr/86Sr values. Earth Planet. Sci. Lett. 463, 310–322. https://doi.org/10.1016/j.epsl.2017.01.034.
- Yu, J., Day, J., Greaves, M., Elderfield, H., 2005. Determination of multiple element/ calcium ratios in foraminiferal calcite by quadrupole ICP-MS: foraminiferal calcite. Geochem. Geophys. Geosyst. 6 https://doi.org/10.1029/2005GC000964 n/a-n/a.
- Zhang, Y., Zhang, Xu, Chiessi, C.M., Mulitza, S., Zhang, Xiao, Lohmann, G., Prange, M., Behling, H., Zabel, M., Govin, A., Sawakuchi, A.O., Cruz, F.W., Wefer, G., 2016. Equatorial Pacific forcing of western Amazonian precipitation during Heinrich Stadial 1. Sci. Rep. 6, 35866. https://doi.org/10.1038/srep35866.
- Zimmermann, M., Meir, P., Silman, M.R., Fedders, A., Gibbon, A., Malhi, Y., Urrego, D. H., Bush, M.B., Feeley, K.J., Garcia, K.C., Dargie, G.C., Farfan, W.R., Goetz, B.P., Johnson, W.T., Kline, K.M., Modi, A.T., Rurau, N.M.Q., Staudt, B.T., Zamora, F., 2010. No differences in Soil Carbon stocks across the tree Line in the Peruvian Andes. Ecosystems 13, 62–74. https://doi.org/10.1007/s10021-009-9300-2.